

Trrap-Dependent Histone Acetylation Specifically Regulates Cell-Cycle Gene Transcription to Control Neural Progenitor Fate Decisions

Alicia Tapias,¹ Zhong-Wei Zhou,¹ Yue Shi,^{2,3} Zechen Chong,^{2,3} Pei Wang,¹ Marco Groth,¹ Matthias Platzer,¹ Wieland Huttner,⁴ Zdenko Herceg,⁵ Yun-Gui Yang,^{2,3} and Zhao-Qi Wang^{1,6,*}

¹Leibniz Institute for Age Research, Fritz Lipmann Institute (FLI), Beutenbergstrasse 11, 07745 Jena, Germany

²Disease Genomics and Individualized Medicine Laboratory, Beijing Institute of Genomics, Chinese Academy of Sciences, 1–7 Beichen West Road, Chaoyang District, Beijing 100101, P.R. China

³University of Chinese Academy of Sciences, 19A Yuquan Road, Beijing 100049, P.R. China

⁴Max Planck Institute of Molecular Cell Biology and Genetics, Pfotenhauerstrasse 108, 01307 Dresden, Germany

⁵International Agency for Research on Cancer (IARC), 150 Cours Albert Thomas, 69008 Lyon, France

⁶Faculty of Biology and Pharmacy, Friedrich Schiller University of Jena, Fuerstengraben 26, 07743 Jena, Germany

*Correspondence: zqwang@fli-leibniz.de

<http://dx.doi.org/10.1016/j.stem.2014.04.001>

SUMMARY

Fate decisions in neural progenitor cells are orchestrated via multiple pathways, and the role of histone acetylation in these decisions has been ascribed to a general function promoting gene activation. Here, we show that the histone acetyltransferase (HAT) cofactor transformation/transcription domain-associated protein (Trrap) specifically regulates activation of cell-cycle genes, thereby integrating discrete cell-intrinsic programs of cell-cycle progression and epigenetic regulation of gene transcription in order to control neurogenesis. Deletion of *Trrap* impairs recruitment of HATs and transcriptional machinery specifically to E2F cell-cycle target genes, disrupting their transcription with consequent cell-cycle lengthening specifically within cortical apical neural progenitors (APs). Consistently, *Trrap* conditional mutants exhibit microcephaly because of premature differentiation of APs into intermediate basal progenitors and neurons, and overexpressing cell-cycle regulators in vivo can rescue these premature differentiation defects. These results demonstrate an essential and highly specific role for *Trrap*-mediated histone regulation in controlling cell-cycle progression and neurogenesis.

INTRODUCTION

During brain development, the number and diversity of neurons and other cell types are determined by multiple cues controlling the proliferation and differentiation of stem and progenitor cells in a spatiotemporal manner (Farkas and Huttner, 2008). The embryonic neocortex is organized into two germinal zones, the ventricular zone (VZ) and the subventricular zone (SVZ). The VZ contains apical progenitors (APs; also termed radial glial cells), which are transformed from the neuroepithelial cells (the neural

stem cells) (Gal et al., 2006; Götz and Huttner, 2005; Kriegstein and Götz, 2003) and divide at the ventricular surface of the VZ (Farkas and Huttner, 2008). The SVZ, localized above the basal layer of the VZ, contains the intermediate or basal progenitors (BPs), which emerge from the APs and divide away from the ventricular surface (Haubensak et al., 2004). Unlike APs that give rise to BPs, neurons, and self-renewal, BPs mainly produce neurons (Noctor et al., 2008). These processes are highly influenced by extrinsic cues, including growth factors, cytokines, adhesion molecules, extracellular matrix, and physical cues that can be sensed through the primary cilia (Han and Alvarez-Buylla, 2010). Equally important, intrinsic programs, such as transcription control and spindle alignment, represent a decisive mechanism in the maintenance and expansion of neural stem and neural progenitor (NP) cells (Fietz and Huttner, 2011; Molyneux et al., 2007; Tiberi et al., 2012). Another cell-intrinsic program regulating NPs output appears to be through cell-cycle progression (Lange et al., 2009; Pilaz et al., 2009).

A tight control of the gene expression profile during development is critical to transform proliferative, undifferentiated tissues into a fully functional brain cytoarchitecture. Growing evidence indicates that epigenetic mechanisms can control transcriptional programs and influence cell fate (Fazzio et al., 2008). The epigenetic modification of histones has emerged as a key player in the brain development and also in the brain functionality in adulthood. The importance of histone acetylation in neural stem cell differentiation has been ascribed to its regulation of the expression of genes in CNS development (Balasubramaniyan et al., 2006; Hsieh et al., 2004; Wang et al., 2010). Furthermore, NPs are shown to preserve their differentiation in the absence of external cues through mechanisms that could involve epigenetic modifications (Ravin et al., 2008; Shen et al., 2006).

Histone acetylation is modulated by histone acetyltransferases (HATs) and histone deacetylases (HDACs). The HAT cofactor transformation/transcription domain-associated protein (Trrap) is a component shared by several HAT complexes, including SAGA, P300/CBP-associated factor (PCAF), and Tip60 (Murr et al., 2007). *Trrap* downregulation or deletion causes cell and mouse lethality, defects in the spindle checkpoint, and differentiation (Herceg et al., 2001; Li et al., 2004;

Loizou et al., 2009; Wurdak et al., 2010). Trrap and other Tip60 complex components are important for the maintenance of the cell status of mouse embryonic stem cells and brain-tumor-initiating cells by regulating stemness genes (Fazio et al., 2008; Sawan et al., 2013; Wurdak et al., 2010). Genetic and chemical inhibition of HDACs resulted in somewhat controversial data regarding the role of histone deacetylation in neural stem cell differentiation (Balasubramaniyan et al., 2006; Montgomery et al., 2009). Thus, the exact mechanisms by which histone acetylation and deacetylation influence differentiation of NPs are not fully understood.

RESULTS

Trrap Deletion Results in Severe Developmental Defects in the Brain

We have previously shown that null mutation of *Trrap* causes early embryonic lethality (Herceg et al., 2001). To overcome the lethality and study the HAT function in neurogenesis, we crossed *Trrap*-floxed mice (*Trrap*^{fl/fl}) with *Nestin-Cre* mice in order to generate mice with *Trrap* deletion in the CNS (*Trrap*^{fl/fl}; *Cre*⁺, termed Trrap-CNSΔ). *Nestin-Cre* expression efficiently deleted *Trrap* in mutant embryonic brains as well as isolated NPs (Figures S1A–S1D available online). Consistent with its role in HAT, *Trrap* deletion resulted in a reduction of global acetylation of histones H3 and H4 (Figures S1E and S1F). *Trrap*^{fl/fl}; *Cre*⁺ mice or *Trrap*^{fl/fl} mice showed no detectable phenotype and thus were used as controls (Co). Trrap-CNSΔ mice developed to term but died at birth. Although the body weight was indistinguishable, the brain weight of Trrap-CNSΔ mice was around 60% of that in Co, reminiscent of microcephaly (Figures 1A and 1B). Histological examination of Trrap-CNSΔ newborn brains (embryonic day [E] 18.5) revealed severe atrophy, characterized by large ventricular cavities and a pronounced decrease in thickness and disorganized layers in the newborn cortex (Figure 1C). Gross abnormalities of Trrap-CNSΔ brain became obvious as early as E15.5, when the ventricles started to become dilated (Figure S1G). At this stage, the Trrap-CNSΔ cortex appeared disorganized and showed a lack of clear separation between the VZ and SVZ (Figure 1D).

Deletion of Trrap Reduces Proliferation and Increases Cell Death in the Neocortex

To investigate possible causes of brain atrophy, we used *in vivo* pulse labeling of bromodeoxyuridine (BrdU) in order to analyze the proliferation of Trrap-CNSΔ NPs. A significantly smaller BrdU⁺ population appeared in E16.5 Trrap-CNSΔ cortices in comparison to controls but not before (i.e., E15.5; Figures 1E and 1F), suggesting either a decreased proliferation or a disappearance of NPs by cell death or premature differentiation. To examine the levels of apoptosis, terminal deoxynucleotidyl transferase dUTP nick end labeling (TUNEL) staining on brain sections at E15.5 detected a significantly increased, albeit a generally low, proportion of TUNEL⁺ cells (~0.61%) in the TrrapΔ cortices in comparison to controls (~0.05%; Figures 1G and 1H).

Mislocalization of NPs in Trrap-CNSΔ Neocortex

Because other knockout mice exhibit a high extent of apoptosis in the developing cortex in the absence of atrophy (Frappart

et al., 2007; Gruber et al., 2011; Shull et al., 2009; Zhou et al., 2012), a relatively modest cell death in Trrap-CNSΔ neocortex is unlikely to fully account for the striking reduction in cortex thickness. Thus, we reasoned whether a depletion of progenitor pools caused the microcephaly. Costaining of the AP marker Pax6 and the BP marker Tbr2 revealed that a mixed localization of BPs and APs with an ectopic presence of BPs was evident in the proliferative area of E15.5 Trrap-CNSΔ cortices (Figure 2A). Additionally, the ratio of BP (Tbr2⁺)/AP (Pax6⁺) was significantly increased in mutants at E15.5 but not E14.5 (Figure 2B).

To determine the reason for the disturbed ratio of BPs versus APs in Trrap-CNSΔ cortex, we took advantage of the fact that APs divide at the apical surface and BPs divide in the SVZ area. We performed immunostaining of the mitotic marker phosphohistone H3 (p-H3) and found an increase of basal p-H3⁺ cells in Trrap-CNSΔ cortex at E15.5 but not earlier (Figures 2A and 2C). However, no significant difference in the number of apical mitoses was observed in Trrap-CNSΔ cortex at both E14.5 and E15.5 (Figure 2C). These results suggest that TrrapΔ APs can divide normally but produce more BPs. To map the identity of these mitotic cells, we coimmunostained p-H3 with Pax6 and Tbr2 (Figure 2A). Notably, in Trrap-CNSΔ cortices, a significant number of basal mitoses expressed only Pax6, representing ectopic AP division (Figure 2D). We also found that a significant proportion of basal mitotic cells lost both Pax6 and Tbr2 markers, which was rarely seen in control neocortex (Figure 2D). Coimmunostaining of p-H3 with Sox2 and Tbr2 showed a similar pattern and a significant increase of basal mitotic cells lacking both Sox2 and Tbr2 markers (Figures S2A and S2B). Although we were unable to identify the nature of this population, these may represent nonneuroprogenitors. We also analyzed the progenitor status in other regions, namely midbrain and hindbrain, that lack basal progenitors. We found no obvious difference of Tbr2⁺ cells and p-H3⁺ cells in basal and apical areas in both control and mutant sections (Figures S2C and S2D). Tuj1 staining revealed a general reduction of the neuronal areas, although the relative thickness was comparable between controls and mutants (Figures S2C and S2E). These results suggest a specific role of Trrap in preventing premature differentiation in cortical progenitors *in vivo*.

Increased Differentiation of APs upon Trrap Deletion

To further analyze whether the increased ratio of BPs versus APs was due to biased production of certain daughter cells from APs, we crossed the Trrap-CNSΔ mice with transgenic mice expressing *Tis21-GFP* that expresses in the subpopulation of APs or BPs committed to producing neurons (Haubensak et al., 2004). We found an enrichment of *Trrap-GFP*⁺Pax6⁺ APs in Trrap-CNSΔ cortices in comparison to controls (Figures 3A and 3B), demonstrating a strong bias of TrrapΔ APs toward neuron commitment. Furthermore, unscheduled differentiation from APs to BPs was assessed by *in utero* electroporation of E14.5 embryos with a vector encoding red fluorescent protein (RFP), allowing us to monitor the fate of RFP⁺ cells after 24 hr. As shown in Figures 3C and 3D, a significantly higher level of RFP⁺Tbr2⁺ cells was detected in Trrap-CNSΔ cortices in comparison to controls. However, the degree of neuronal differentiation of BPs (*Trrap-GFP*⁺Tbr2⁺) was not significantly different between control and Trrap-CNSΔ cortices (Figures 3E and 3F), suggesting that Trrap

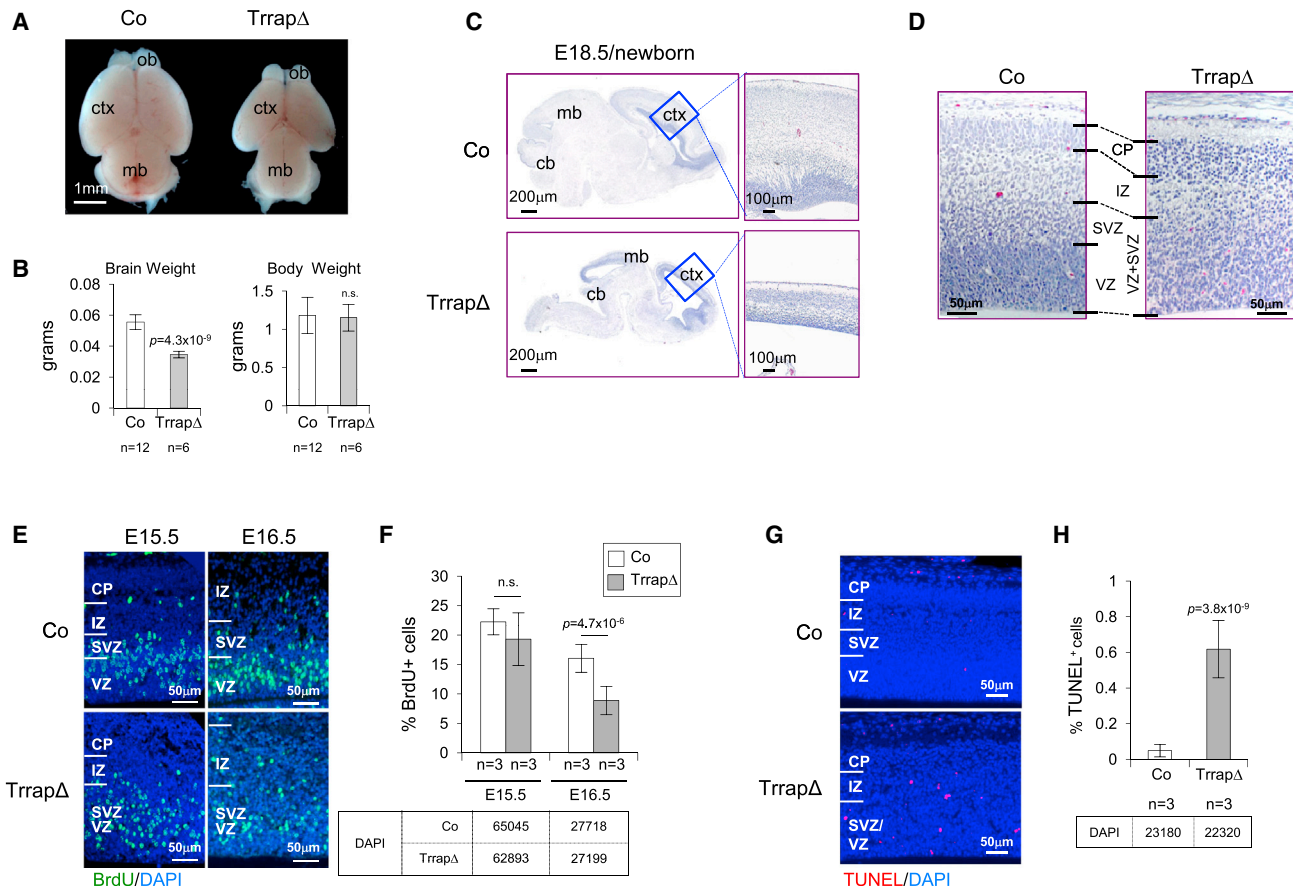


Figure 1. Deletion of Trrap in the CNS Causes Severe Brain Atrophy

(A) Dorsal view of E18.5/newborn brains.
 (B) Brain and body weight of newborn mice.
 (C) H&E staining of sagittal sections from control and Trrap-CNSΔ E18.5/newborn brains. Note a pronounced reduction of the cortex thickness in Trrap-CNSΔ brains. Enlarged views of the E18.5 cortical area are depicted on the right.
 (D) H&E staining of sagittal sections from control and Trrap-CNSΔ E15.5 embryonic cortex.
 (E) Immunostaining of E15.5 and E16.5 embryonic cortex with a BrdU antibody (green) and counterstained with DAPI (blue).
 (F) Quantification of the percentage of BrdU⁺ cells among the total DAPI⁺ cells.
 (G) TUNEL reaction (red) was conducted on E15.5 sagittal sections followed by DAPI counterstaining (blue).
 (H) Quantification of the percentage of apoptotic cells (TUNEL⁺) among the total DAPI⁺ cells in E15.5 neocortex.
 Total numbers of cells analyzed are indicated in the tables below the histograms. n = number of embryos analyzed. Mean ± SEM is shown. A Student's t test was performed for statistical analysis. n.s., not significant; Co, control; TrrapΔ, Trrap-CNSΔ; Ob, olfactory bulb; ctx, cortex; mb, midbrain; cb, cerebellum; CP, cortical plate; IZ, intermediate zone; SVZ, subventricular zone; VZ, ventricular zone.
 See also [Figure S1](#).

deletion does not affect the fate of BPs nor BP self-renewal. Given that different cyclin Ds operate in AP and BP populations, we costained cyclin D1 or D2 with Sox2 or Tbr2, respectively. Interestingly, deletion of Trrap resulted in an increase of the Tbr2⁺cyclin D1⁺ as well as Sox2⁺cyclin D2⁺ populations (Figures S2F and S2G). These two populations could both represent apical progenitors that are about to or have just become basal progenitors (Glickstein et al., 2007, 2009), indicative of an increased differentiation of APs to BPs. Altogether, Trrap deletion specifically promotes differentiation of APs to BPs and neurons.

Next, we investigated whether Trrap deletion would alter the orientation of mitotic spindles to influence the NP self-renewal or differentiation. We examined the cleavage planes of mitotic APs and found no significant difference between control and

mutant APs in the distribution of the apical plasma membrane harboring the cadherin hole in the endfoot (Figures S3A and S3C). Moreover, the orientation of the mitotic spindle was not affected by the Trrap deletion (Figures S3B and S3C). These data indicate that the premature differentiation of TrrapΔ APs is unlikely resulted from changes in the spindle orientation of APs.

Premature Differentiation of Trrap-Δ NPs In Vitro

To test whether premature differentiation of TrrapΔ NPs was cell autonomous or influenced by external cues, we isolated NPs from E14.5 brains in order to form neurospheres in culture. Although no significant difference in the total number of neurospheres was observed between TrrapΔ and control brains, the

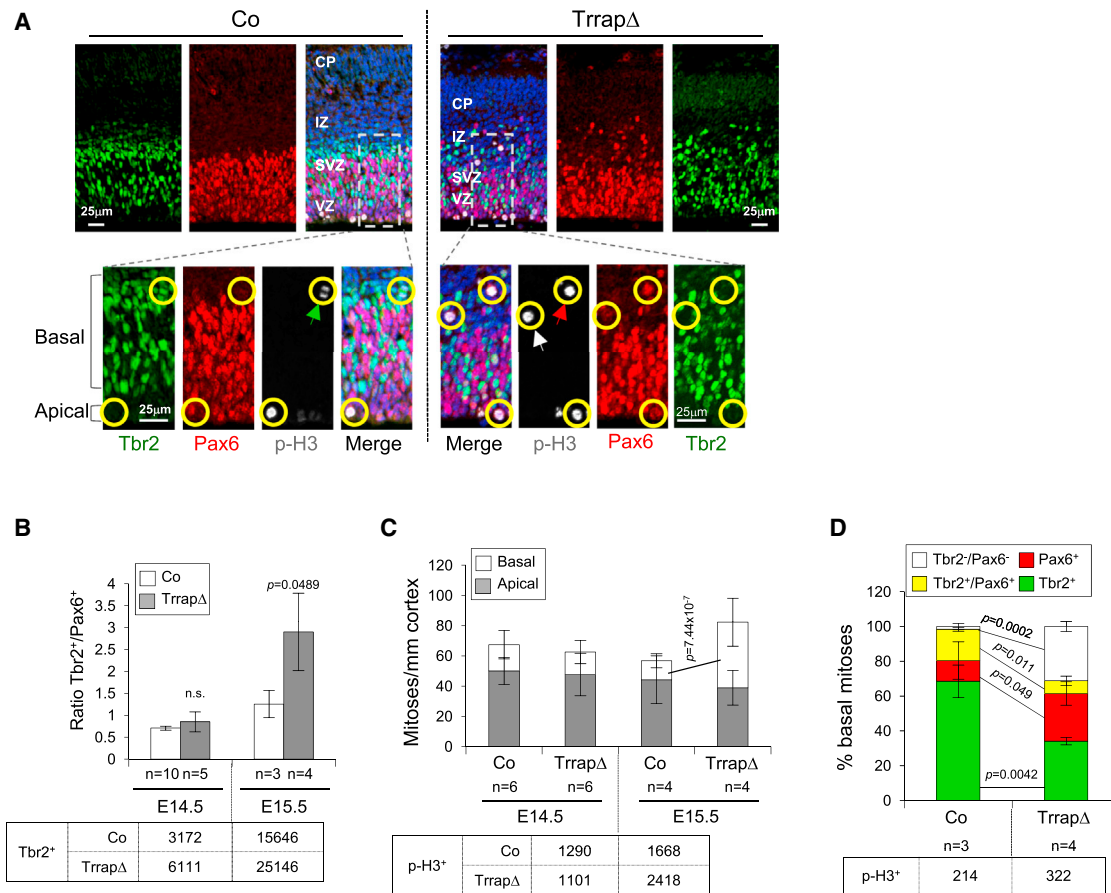


Figure 2. Trrap Deletion Changes the Division of NPs

(A) Coronal sections of E15.5 embryos were stained against AP marker Pax6 (red), BP marker Tbr2 (green), and mitotic marker p-H3 (white) and counterstained with DAPI (blue). Yellow circles indicate mitotic cells, the red arrow denotes Pax6⁺Tbr2⁻ basal mitosis, the green arrow indicates Tbr2⁺Pax6⁻ mitosis, and the white arrow denotes Tbr2⁻Pax6⁻ mitosis. Double Tbr2⁺Pax6⁺ mitosis is not shown.

(B) Quantification of the progenitor populations at E14.5 and E15.5 expressed as a ratio of BPs to APs (Tbr2⁺/Pax6⁺).

(C) Quantification of apical and basal mitoses in E14.5 and E15.5 embryonic cortices is shown.

(D) Percentile composition of basal mitotic cells at E15.5 expressing Pax6 and Tbr2 markers, either alone or in combination.

Total numbers of cells analyzed are indicated in the tables below the histograms. n = number of embryos analyzed. Mean ± SEM is shown. A Student's t test was performed for statistical analysis. n.s., not significant; Co, control; TrrapΔ, Trrap-CNSΔ; CP, cortical plate; IZ, intermediate zone; SVZ, subventricular zone; VZ, ventricular zone.

See also Figure S2.

number of cells in each neurosphere was 10-fold lower in Trrap-CNSΔ than controls (Figures 4A–4C). TrrapΔ NPs were unable to form secondary neurospheres. These findings indicate that TrrapΔ NPs possess a highly compromised self-renewal capacity. Strikingly, immunofluorescence staining of NP cultures revealed a spontaneous neuronal differentiation of TrrapΔ neurospheres judged by a high proportion of Tuj1⁺ cells (Figures 4D and 4E). Moreover, NPs derived from the cortex, midbrain, hindbrain, or ganglionic eminences all showed a premature differentiation of NPs to neurons (Figure 4F). These data indicate that loss of Trrap promotes the premature differentiation of NPs in a cell-autonomous manner. However, we did not detect an increase of the relative Tuj1⁺ population in all these regions of TrrapΔ brains in vivo (see Figures S2C–S2E), which could be attributed to a lower proliferation rate of TrrapΔ NPs and increased apoptosis of TrrapΔ neurons.

Trrap Controls the Expression of Cell-Cycle Regulators in NPs

Trrap recruits HAT activity to target promoters and assist transcriptional initiation (Murr et al., 2007). To analyze the possible causes of the unscheduled differentiation of APs, we conducted a genome-wide analysis of mRNA levels (RNA sequencing [RNA-seq]) with three biological replicates from E14.5 cortices. Trrap deletion resulted in highly reproducible changes in the transcriptome of cortices with 2,381 genes whose expression showed a significant change (false discovery rate adjusted p value defined by Cufflinks, q < 0.05; NCBI Gene Expression Omnibus [GEO] number GSE43650; Figure 5A) (Trapnell et al., 2012). Moreover, transcriptional levels in control and Trrap-CNSΔ cortices were highly correlated (Pearson correlation coefficient r² = 0.8339; p < 0.0001; Figure 5B), indicating that the global transcriptional activity did not change because of Trrap deletion. Bioinformatic

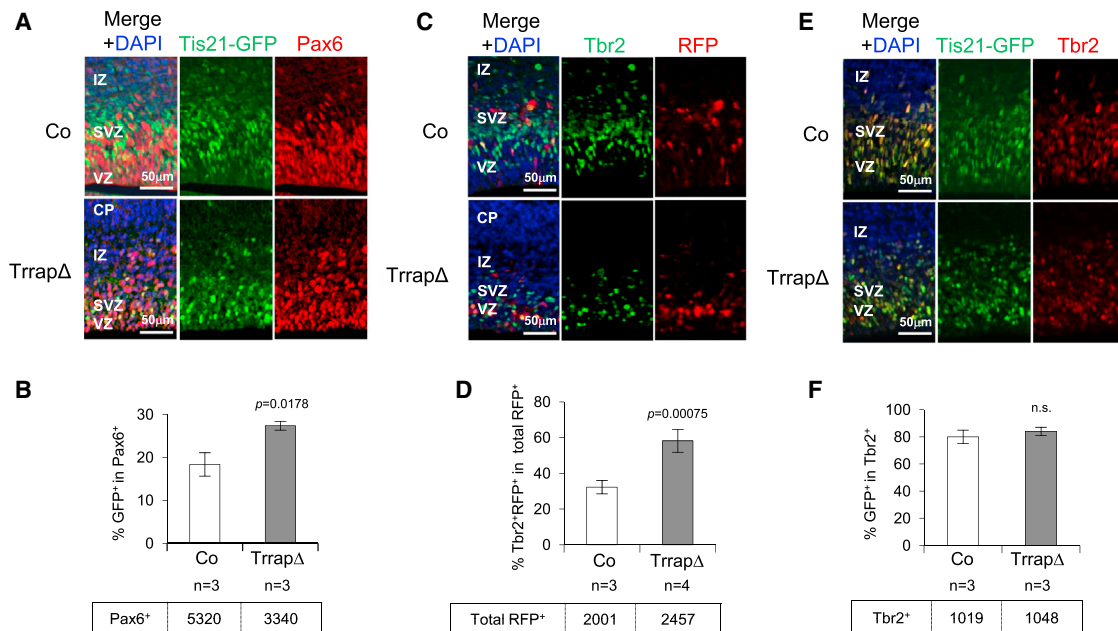


Figure 3. Trrap Deletion Promotes AP Differentiation

(A) Coronal sections of E15.5 embryos expressing Tis21-GFP transgene (green) were stained with Pax6 antibody (red) and counterstained with DAPI (blue). (B) Percentage of APs (Pax6⁺) undergoing neurogenic commitment (Tis21-GFP⁺) among all Pax6⁺ cells. (C) E14.5 embryos were electroporated in utero with an expression vector for RFP (red) in order to allow labeling of APs. E15.5 coronal sections were stained with the BP marker Tbr2 (green) and counterstained with DAPI (blue). (D) Quantification of RFP⁺ cells that coexpress Tbr2 derived from all RFP-transfected APs in a period of 24 hr. (E) Coronal sections of E15.5 embryos expressing Tis21-GFP transgene (green) were stained with Tbr2 (red) and counterstained with DAPI (blue). (F) Percentage of BPs (Tbr2⁺) undergoing neurogenic commitment (Tis21-GFP⁺) among all Tbr2⁺ cells. Total numbers of cells analyzed are indicated in the tables below the histograms. n = number of embryos analyzed. Mean ± SEM is shown. A Student's t test was performed for statistical analysis. n.s., not significant; Co, control; TrrapΔ, Trrap-CNSΔ; CP, cortical plate; IZ, intermediate zone; SVZ, subventricular zone; VZ, ventricular zone. Related to Figure S3.

analysis revealed that the most affected pathways upon *Trrap* deletion were ribosomal genes followed by the cell-cycle-regulation group (Figures 5C and S4A and Table S1). Notably, the ribosomal genes group contained about 50% of pseudogenes and predicted genes ($p = 4.5 \times 10^{-45}$). Additionally, genes involved in neuronal maturation and axon guidance were found to be downregulated upon *Trrap* deletion (Figures 5C and S4A and Table S1). In agreement with the increase in neurogenesis (premature differentiation), genes involved in axon growth and synaptic transmission were also enriched upon *Trrap* deletion (Figure S4B and S4C and Table S1). Notably, the neurogenesis master genes, such as Notch, Wnt, BMP, and epidermal growth factor (EGF) signaling, as well as Pax6 and Tbr2, were not dysregulated (Figures 5C and S4), suggesting that the primary cause of the premature differentiation of *Trrap*-CNSΔ progenitors is most likely independent of these pathways. Thus, we considered the cell-cycle regulation as one of the most relevant pathways involved in the unscheduled differentiation of *Trrap* NPs.

Deletion of *Trrap* Lengthens Cell-Cycle Progression of NPs in the Neocortex

To further investigate whether the change of cell fate in APs could be a consequence of impaired cell-cycle progression, we measured in vivo the cell-cycle parameters of *Trrap*Δ NPs

with a cumulative 5-ethynyl-2'-deoxyuridine (EdU) incorporation assay (Arai et al., 2011) in conjunction with immunostaining for Pax6 and Tbr2, respectively (Figures S5A and S5B). *Trrap* deletion dramatically elongated the total cell-cycle length within the AP population (42.3 versus 21.1 hr), whereas only a modest delay was found in the BP population (29.7 versus 24.6 hr). The growth curve of *Trrap*Δ APs did not reach a plateau, indicative of incompleteness of cell cycle by most cells in the cortices, even 30 hr after the first EdU injection (Figure 6A). Next, we combined EdU labeling and immunostaining for p-H3 in order to measure the duration of G2 and M phases of NPs within 7 hr after the first EdU injection (Figures S5A and S5C). The coappearance of EdU labeling and p-H3 signal (as a mitotic EdU-labeling index) is a measure of half of G2 phase length. The duration of the G2 and M phases was about 2-fold longer in *Trrap*Δ APs and about 1.5-fold longer in *Trrap*Δ BPs (Figures 6B and 6C). On the basis of the time duration of EdU labeling of a total of 30 hr in conjunction with G2 and M phase length, we calculated the lengths of G1 and S phases. *Trrap*Δ APs (Pax6⁺) showed approximately 2-fold elongation in S and G1 phases, whereas these phases of BPs (Tbr2⁺) were not significantly changed (Figure 6C). To further study the differential response of APs and BPs in *Trrap*Δ neocortex, we stained control cortices with antibodies against Gcn5, a HAT-containing *Trrap*, or CBP, a *Trrap*-independent

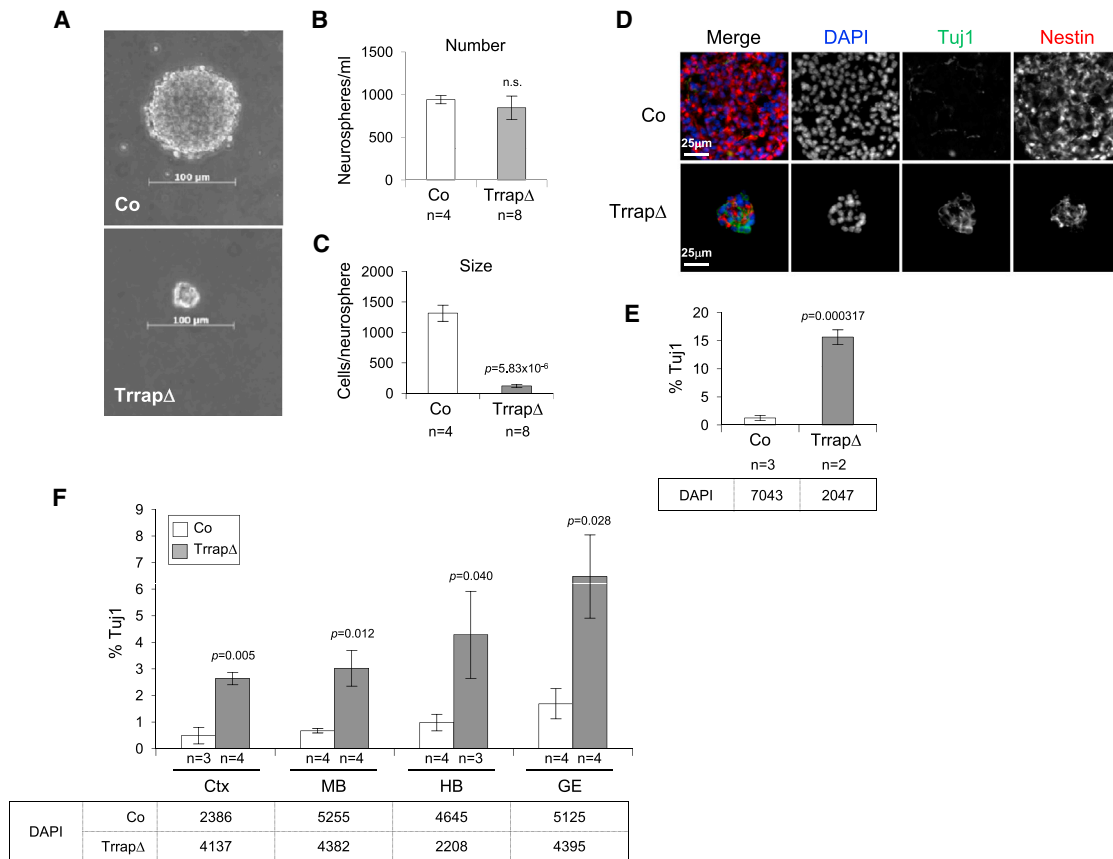


Figure 4. Characterization of Trrap-Deficient NPs In Vitro

(A) Representative primary neurospheres formed after 7 days in culture.

(B and C) An equal number (8×10^4 cells/ml) of dissociated E14.5 brain cells were plated. The number of neurospheres per ml (B) and the number of cells per neurosphere (C) were quantified after 7 days in culture.

(D) Neurospheres were cryosectioned and immunostained using antibodies against progenitor marker Nestin (red) and neuronal marker β -tubulin III/Tuj1 (green). (E) NPs were plated at a 15,000 cells/cm² density in polylysine- and laminin-coated plates 4 days after isolation. Cells were fixed after 4 days and immunostained with β -tubulin III/Tuj1 antibody. Quantification of Tuj1⁺ cells among the total cell number is shown.

(F) Neurospheres isolated from the indicated areas of the E14.5 embryonic brain were plated at a 30,000 cells/cm² density in polylysine- and laminin-coated plates 3 days after isolation. Cells were fixed after 3 days and immunostained with β -tubulin III/Tuj1 antibody. Quantification of Tuj1⁺ cells among the total cell number is shown.

Total numbers of cells analyzed are indicated in the tables below the histograms. n = number of embryos analyzed. Mean \pm SEM is shown. A Student's t test was performed for statistical analysis. n.s., not significant; Co, control; TrrapΔ, Trrap-CNSΔ; Ctx, cortex; MB, midbrain; HB, hindbrain; GE, ganglionic eminence.

HAT. Strikingly, whereas CBP exhibited a uniform expression pattern along the cortex, Gcn5 expression was enriched in the VZ, where the APs are located (Figure 6D). These findings argue for a specific role of Trrap-containing HATs in APs.

Trrap Regulates E2F Targets during Cell-Cycle Progression of NPs

The transcription factor E2F1 directly binds Trrap in order to recruit HAT complexes to target genes and is a regulator of cell-cycle progression (Lang et al., 2001; McMahon et al., 1998; Taubert et al., 2004). Comparison of known E2F targets (Bracken et al., 2004) with the list of differentially expressed genes (DEGs) derived from TrrapΔ cortices (Table S2) revealed that a group of downregulated cell-cycle regulators were E2F targets (Figure S6A). We also analyzed by immunoblotting the E2F targets E2F3, Cdc25A, and Plk1 (from the RNA-seq

screening), and Mad2 and cyclin A2 (derived from the literature as E2F targets) with cortices and purified NPs that minimize the influence by other cell types. We found a downregulation of all E2F targets, but not E2F1, in TrrapΔ NPs and cortex extracts in comparison to controls (Figures 7A and S6B). These results confirm that E2F targets are indeed regulated by Trrap during neurogenesis.

To gain additional insight into the molecular mechanisms underlying the decrease of E2F targets, we performed chromatin immunoprecipitation (ChIP) on the promoter of Cdc25A in order to analyze the binding of transcription factors (E2F1 and E2F3), RNA polymerase, and HATs (Tip60, Gcn5, and PACF) and found much reduced enrichment of binding by these factors in chromatin purified from TrrapΔ NPs (Figure 7B). We also observed downregulation of Ach3 and Ach4 in the Cdc25A promoter (Figure 7B). Furthermore, the binding of E2F1, Tip60, Gcn5, and

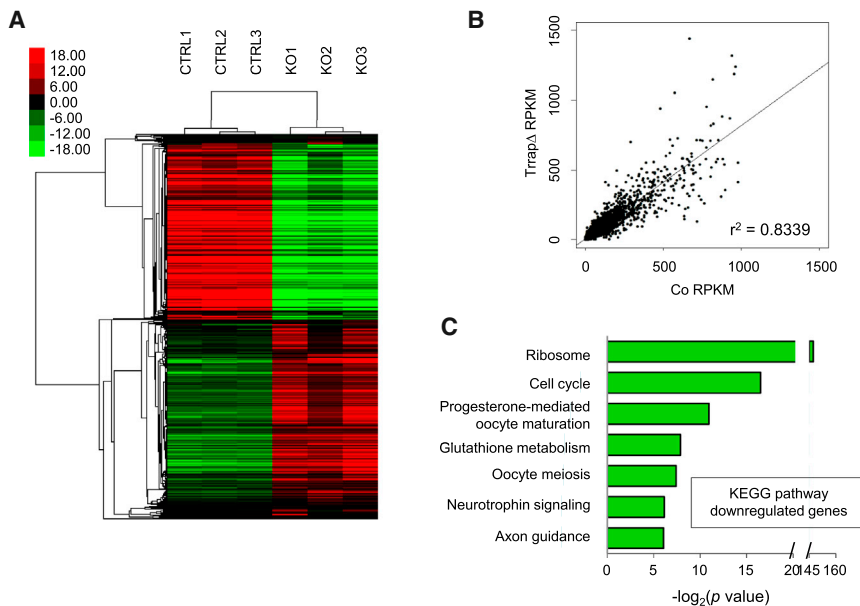


Figure 5. Transcriptome Analysis of *Trrap*-CNS Δ Cortices

(A) Gene expression cluster analysis of DEGs upon *Trrap* deletion. From a total of 2,381 DEGs, 2,189 were subjected to analysis. SD < 0.5.

(B) Correlation of relative expression values of RNA-seq between *Trrap*-CNS Δ and control E14.5 cortices. Comparison of reads per kilobase per million mapped reads (RPKM) values from RNA-seq libraries generated from *Trrap*-CNS Δ and control cortices demonstrates a strong positive correlation ($r^2 = 0.8339$, $p < 0.0001$).

(C) KEGG pathway enrichment analysis of the significantly ($q < 0.05$) downregulated genes. Overrepresented KEGG pathways for genes that are downregulated in *Trrap*-CNS Δ cortices are shown in the histogram.

Co/CTRL, control; KO/*Trrap* Δ , *Trrap*-CNS Δ .

See also Figure S4 and Table S1.

PCAF to the promoter of *Mad2*, *cyclin A2*, and *Top2A* was also severely impaired in *Trrap* Δ NPs (Figures 7C–7E). These results demonstrate that *Trrap*-mediated recruitment of HAT activity is indeed important for the transcriptional regulation of E2F targets. To test whether *Trrap* is essential for the activation of E2F target genes in NPs, we transfected an E2F1-expressing vector into NPs and detected an efficient upregulation of the target gene *Top2A* in control NPs, which was repressed in *Trrap* Δ NPs (Figures S7A and S7B), indicating a *Trrap* dependence of E2F1-mediated transcriptional activation. These results suggest that downregulation of E2F-targeted cell-cycle regulators is a direct consequence of the lack of *Trrap*-dependent modulation of E2F on specific promoters.

To ultimately investigate whether the downregulation of these cell-cycle regulators was indeed responsible for the premature differentiation of NPs, we performed in utero electroporation in order to ectopically express mCherry along with cyclins A2 and B1, both of which are E2F targets and downregulated in *Trrap*-CNS Δ cortices (see Table S2 and Figure S6A). Intriguingly, ectopic expression of cyclin A2 alleviated neuronal overproduction of NPs because there was a significant decrease of the progenitors coexpressing mCherry and *Tis21*-GFP in *Trrap*-CNS Δ cortices (Figures 7F and 7G). Overexpression of cyclin A2 also reduced AP to BP differentiation, as judged by depletion of mCherry⁺Tbr2⁺ populations, albeit lacking a strong statistical significance (Figures 7F and 7H). Notably, co-overexpression of cyclins B1 and A2 significantly rescued the unscheduled differentiation of APs to neurons and to BPs (Figures 7G and 7H), suggesting that *Trrap*-HAT modulates NP differentiation through the cell-cycle control.

DISCUSSION

The fate determination of NPs, orchestrated by intrinsic and extrinsic mechanisms, is fundamental for the achievement of the fine brain architecture. Histone acetylation in concert with

other epigenetic mechanisms modulates NP cell fate by transcription regulation of neural genes (Hirabayashi and Gotoh, 2010; Juliandi et al., 2010). Here, we show that *Trrap*-dependent histone acetylation modulates the differentiation route of APs to BPs and neurons during cortical neurogenesis through the modulation of a subset of E2F targets that regulates cell-cycle length.

We have previously shown that constitutive knockout of *Trrap* results in cell lethality (Herceg et al., 2001; Li et al., 2004). Surprisingly, the cell-death program seems to operate differently in neural cells because cell death became evident only at E14.5 (A.T., unpublished data) despite the fact that *Trrap* deletion occurs efficiently at E12.5. During this period, APs should divide at least five times in vivo (Arai et al., 2011; Takahashi et al., 1999). Nevertheless, an increased apoptosis (~0.61%) in the E15.5 cortex could not fully account for the block of expansion of *Trrap* Δ brains because massive apoptosis in developing brains do not always associate with brain atrophy (Frappart et al., 2007; Gruber et al., 2011; Shull et al., 2009; Zhou et al., 2012). The current study demonstrates that proficient *Trrap*-HAT is a cell-intrinsic mechanism that prevents a premature AP differentiation into BPs and neurons (Figures 3 and 4), which otherwise ultimately reduces the output of the total cell population. Similarly, the CNS conditional knockout of *Gcn5* reduced neuroprogenitor proliferation and increased oligodendrocyte differentiation (Martínez-Cerdeño et al., 2012). However, PCAF knockout mice showed no obvious neurodevelopmental defects but only memory deficits in adulthood (Maurice et al., 2008; Yamauchi et al., 2000). Moreover, heterozygous mutation and small interfering RNA (siRNA) knockdown of the *Trrap*-free HAT cREB binding protein (CBP) inhibits NP differentiation (Alarcón et al., 2004; Wang et al., 2010). On the other hand, HDAC inhibition stimulates the expression of differentiation genes and increases the neuronal production of embryonic and adult neural stem cells (Balasubramaniyan et al., 2006; Hsieh et al., 2004; Juliandi et al., 2012; Zhang et al., 2011). Due to the redundancy, only double knockout of HDAC1 and HDAC2 result in brain atrophy because of a block of NP differentiation (Montgomery et al., 2009; Price et al., 2013). Despite lacking

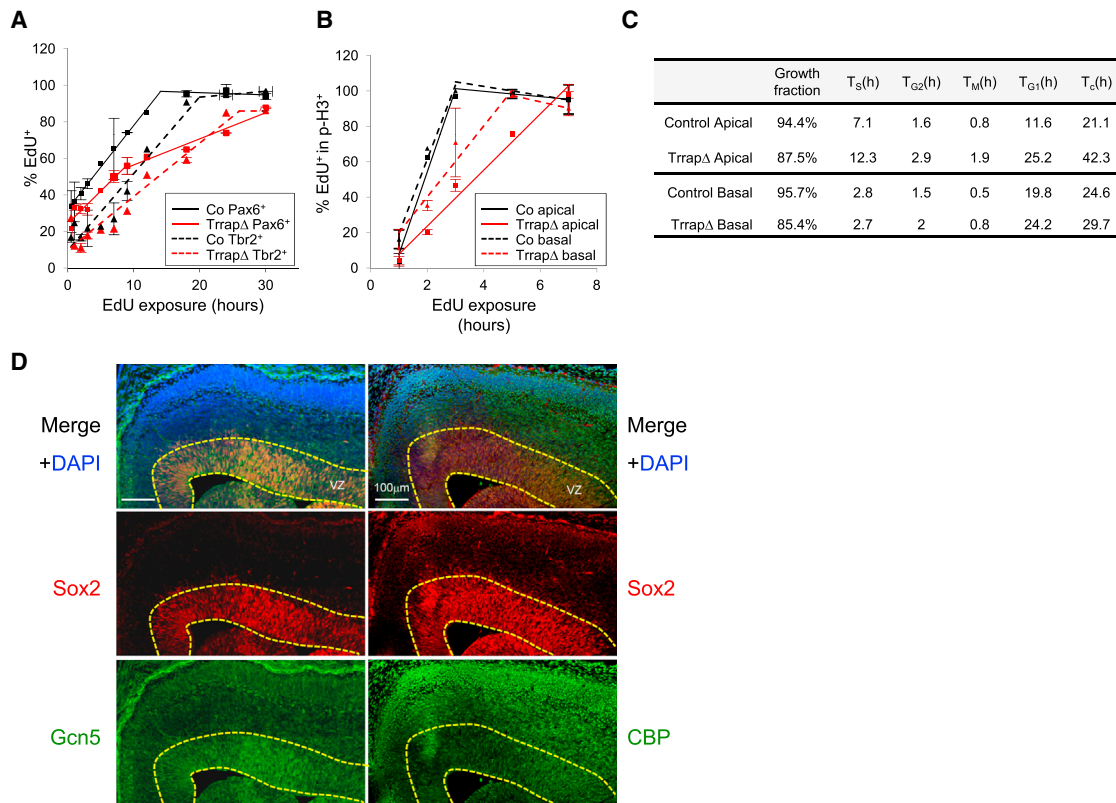


Figure 6. Cell-Cycle Measurement of Trrap Δ NPs In Vivo

(A) Cumulative EdU-labeling curves of Pax6⁺ and Tbr2⁺ cells in control and Trrap-CNS Δ neocortices after labeling for a period of up to 30 hr. The graph shows the percentage of EdU⁺ cells among the indicated population (Pax6⁺ or Tbr2⁺ cells).

(B) Proportion of EdU-labeled mitotic cells (EdU⁺p-H3⁺) within the apical or basal areas after cumulative EdU labeling within a period of 7 hr.

(C) Cell-cycle parameters of APs (Pax6⁺) and BPs (Tbr2⁺) of E14.5 embryos. The cell-cycle phases were calculated from the data of (A) and (B) according to [Arai et al. \(2011\)](#). Time is indicated in hours (h). T_C , total cell cycle; T_{G1} , G1 phase; T_{G2} , G2 phase; T_M , M phase; T_S , S phase.

(D) Coronal sections from control brains were immunostained with antibodies against the AP marker Sox2 (red) and the HATs Gcn5 (left, green) or CBP (right, green). Representative pictures are depicted showing an enrichment of Gcn5 staining in VZ. Yellow lines delineate the VZ as determined by Sox2 staining. Control, n = 23; mutant, n = 21 (A–C). Mean \pm SEM is shown in (A) and (B). Co, control; Trrap Δ , Trrap-CNS Δ .

See also [Figure S5](#).

embryonic brain phenotype, HDAC2 deletion affected adult neurogenesis, suggesting that HDACs may play a distinct role in adult and embryonic neurogenesis ([Jawerka et al., 2010](#)). Rather, these different outcomes highlight the specificity and complexity of histone modifications by HAT or HDAC.

Perhaps the most important event in neurogenesis is the spatiotemporal expression of neural genes that dictates the balance between self-renewal and differentiation of NPs ([Molyneaux et al., 2007](#)). Surprisingly, the major pathways involved in neurogenesis, such as Pax6, Wnt, SHH, etc., were not found to be significantly changed in the Trrap Δ neocortex ([Figure S4](#) and [Table S1](#)). Importantly, our experiments highlight the down-regulation of several key cell-cycle regulators, which causes a dramatic lengthening of all cell-cycle phases in Trrap Δ APs, as the major cause of premature differentiation of NPs, consistent with the notion that elongation of the cell cycle increases NP differentiation ([Lange and Calegari, 2010](#)). Intriguingly, reover-expression of cyclins A2 and B1 could reverse the premature differentiation phenotype of Trrap Δ NPs. Notably, Trrap deletion had a markedly lesser impact on BPs cell-cycle lengthening,

which may attribute to distinct regulatory mechanisms in APs and BPs, for example, because of a specific expression pattern of Gcn5 and CBP in the VZ ([Figure 6D](#)).

The specificity of Trrap in neurogenesis may be dependent on the context of the subunits in the HAT complex ([Lee and Workman, 2007](#)). Notably, differential expression of E2F factors was found between the VZ and the SVZ ([Ayoub et al., 2011](#); [Fietz et al., 2012](#)). Interestingly, we showed that Trrap-HAT-dependent cell-cycle regulation in NPs is mediated by E2F function. Although E2F1-deficient mice show a significant decrease of adult neurogenesis ([Cooper-Kuhn et al., 2002](#)), these mice are devoid of a strong neuronal phenotype, most likely because of functional redundancy of other family members ([Tsai et al., 2008](#)). Although E2F1 expressed normally in Trrap Δ NPs, Trrap deletion decreased E2F1 and E2F3 binding to the target promoters and concomitantly compromised recruitment of HAT complexes and histone acetylation ([Figures 7B–7E](#)), which is line with the role of Trrap in E2F1 binding and recruitment of HAT to target promoters ([Lang et al., 2001](#); [McMahon et al., 1998](#); [Taubert et al., 2004](#)). Also consistent with previous reports

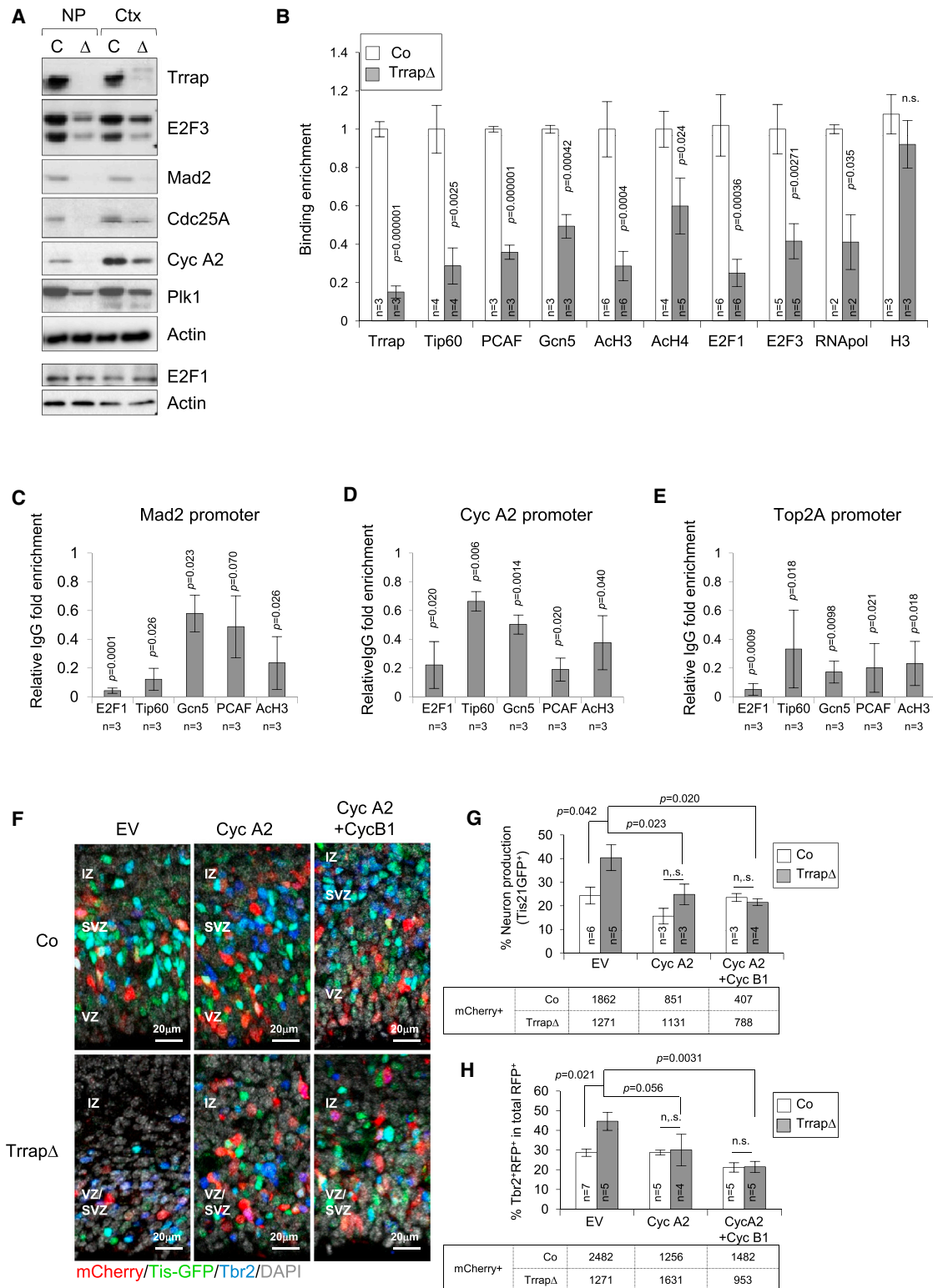


Figure 7. Loss of Trrap Compromises Recruitment of HAT and E2F to the Promoters of Cell-Cycle Regulators in NPs

(A) Immunoblot analysis of E2F targets in isolated E14.5 NPs and E15.5 cortices (Ctx). β -Actin was used as loading control.

(B) ChIP analysis of the *Cdc25A* promoter in E14.5 NPs with the indicated antibodies. qPCR analysis was used to quantify the binding of the indicated factors to the promoter. Binding was calculated as fold enrichment over IgG. The histogram shows the fold enrichment over binding in control NPs for each factor.

(legend continued on next page)

(Dugan et al., 2002; Wurdak et al., 2010), not all E2F targets were affected in the same way upon Trrap deletion (Table S2). This target selectivity may reflect different chromatin configurations in different gene loci and in different cell types (Lee and Workman, 2007; Taubert et al., 2004). Thus, the subset of E2F targets regulated by Trrap in NPs constitutes a program for dictating AP specification.

In the present study, we show that Trrap-HAT specifically regulates cell-cycle genes via E2F in order to maintain the balance between self-renewal and differentiation of NPs in the neocortex. This mechanism guarantees the neuron number output by progenitors during brain development and ultimately determines brain size. Because histone acetylation disturbance accelerates embryonic NP differentiation, future studies are encouraged to an intervention of adult neural stem cells by modulating histone (de)acetylation status, which may have a major impact on the maintenance of the self-renewal capacity of adult neural stem cells during neurodegeneration and regeneration.

EXPERIMENTAL PROCEDURES

Mice

Mice carrying the conditional (floxed, *Trrap*^{fl}) allele (Herceg et al., 2001) were crossed with *nestin*-Cre transgenic mice (Betz et al., 1996) in order to generate mice with a specific deletion in the CNS (Trrap-CNSΔ). *Tis21*-GFP knockin mice (Haubensak et al., 2004) were intercrossed with Trrap-CNSΔ mice. All animal experiments were conducted according to German animal welfare legislation. The Trrap and Cre genotypes of mice were determined by PCR on DNA extracted from tail tissue as previously described (Loizou et al., 2009).

Histology

Tissues for histology were fixed in 4% paraformaldehyde (PFA), processed, and embedded in paraffin wax. For cryosections, tissues were fixed in 4% PFA, cryoprotected in 30% sucrose, and frozen in Richard-Allan Scientific Neg-50 Frozen Section Medium (Thermo Scientific). Sections (thickness of 5–15 μm) were stained with hematoxylin and eosin (H&E) or were used for immunofluorescence staining.

BrdU and EdU Labeling

For single-pulse BrdU labeling, pregnant mice at defined pregnancy stages were injected intraperitoneally with 50 μg/g body weight of BrdU (Sigma-Aldrich) and sacrificed 1 hr after injection. Cumulative EdU labeling was conducted as previously described (Arai et al., 2011).

TUNEL Reaction, EdU Staining, and Immunofluorescence Staining of Brain Sections

TUNEL reaction was conducted on cryosections as previously described (Gruber et al., 2011). Immunofluorescence and EdU staining were performed on 12 μm cryosections prepared from PFA-fixed brains of indicated developmental stages. For Pax6 immunodetection, a Cy3 trichostatin A kit (PerkinElmer) was used as previously described (Arai et al., 2011). BrdU stain-

ing on cryosections was performed as previously described (Gruber et al., 2011). EdU staining was conducted on cryosections with a Click-iT EdU Alexa Fluor 647 Imaging Kit (Life Technologies) according to the manufacturer's instructions. In all cases, sections were counterstained and mounted with Prolong Gold Antifade Reagent (Life Technologies). A list of the antibodies used is provided in the Supplemental Experimental Procedures.

Analysis of Cell-Cycle Parameters

The lengths of the cell-cycle phases were calculated by a nonlinear regression analysis of the cumulative and mitotic EdU labeling indices as previously described (Arai et al., 2011; Gruber et al., 2011; Nowakowski et al., 1989).

In Utero Electroporation

In utero electroporation was performed as previously described (Gruber et al., 2011). RFP and mCherry overexpressing vectors were obtained from Life Technologies; human cyclin A2 and B1 expression vectors were constructed by subcloning the human cyclin A2 and B1 cDNAs into the pcDNA3 vector (Life Technologies). Vectors were injected into the lateral ventricle of E14.5 embryos. Embryos were isolated 24 or 30 hr after electroporation and processed for immunostaining.

Neurosphere Culture and Immunofluorescence Staining

NPs were isolated from E14.5 cortices as previously described (Frappart et al., 2005; Gruber et al., 2011). Adherent NP cultures were derived from primary neurospheres after a maximum of 4 days. Adherent cultures were grown in neurobasal medium supplemented with B27, penicillin and streptomycin, 1% glutamine (200 mM), 1% N-2 supplement (all from Life Technologies), 20 ng/ml EGF, and 10 ng/ml basic fibroblast growth factor (PeproTech). For immunofluorescence staining, NPs were plated onto laminin- and poly-D-lysine-coated coverslips (Sigma-Aldrich). Cryosections of neurospheres were prepared as previously described (Pacey et al., 2006). In brief, neurospheres were suspended in 30% sucrose overnight at 4°C followed by embedding into Richard-Allan Scientific Neg-50 Frozen Section Medium. Cryosectioned neurospheres or adherent cultures were fixed in 4% PFA for 10 min.

Immunoblot Analysis

Total protein lysates were prepared from brain tissue or NPs with RIPA buffer (50 mM Tris-HCl [pH 7.4], 150 mM NaCl, 1% NP40, 0.25% Na-deoxycholate, 1 mM EDTA, 1 mM PMSF, and cComplete Mini Protease Inhibitor Cocktail [Roche Applied Science]), and immunoblotting was performed as previously described (Frappart et al., 2005).

ChIP

ChIP was performed with a LowCell# ChIP Kit (Diagenode) according to the manufacturer's instructions. Chromatin used for immunoprecipitation was isolated from NPs in culture and sonicated with a Bioruptor Plus (Diagenode). Samples obtained from ChIP were analyzed by quantitative PCR (qPCR) with Platinum SYBR Green qPCR SuperMix-UDG (Life Technologies) and a LightCycler 480 Real-Time PCR System (Roche Applied Science). For quantification of the qPCR data, the fold enrichment method was used expressing the results as the enrichment of the binding of a given factor in comparison to the binding of the nonspecific IgGs to the chromatin. A list of primers is provided in the Supplemental Experimental Procedures.

(C–E) ChIP analysis in E14.5 NPs with the indicated antibodies of the promoter of *Mad2* (C), *cyclin A2* (D), and *Top2A* (E) in Trrap-CNSΔ and control cortices. Binding was calculated as fold enrichment over IgG. The histogram shows the fold enrichment over binding in control NPs.

(F) *Tis21*GFP-containing (green) E14.5 embryos were electroporated in utero with an expression vector for mCherry (red) along with the indicated expression vectors. E15.5 coronal sections were stained with an antibody against Tbr2 (blue) and counterstained with DAPI (gray).

(G) Quantification of mCherry⁺ cells that coexpress *Tis21*GFP derived from all mCherry-transfected APs in a period of 30 hr representing the amount of NPs with neurogenic commitment.

(H) Quantification of mCherry⁺ cells that coexpress Tbr2 derived from all mCherry-transfected APs in a period of 30 hr representing the amount of APs differentiated to BPs.

Total numbers of cells analyzed are indicated in the tables below the histograms. n = number of embryos analyzed. Mean ± SEM is shown. A Student's t test was performed for statistical analysis. n.s., not significant; Co, control; TrrapΔ, Trrap-CNSΔ; NP, isolated neuroprogenitors; ctx, cortex; CP, cortical plate; IZ, intermediate zone; SVZ, subventricular zone; VZ, ventricular zone; EV, empty vector.

See also Figures S6 and S7 and Table S2.

RNA-Seq and Data Analysis

RNA was isolated from E14.5 cortices with an RNeasy Lipid Tissue Mini Kit (QIAGEN). RNA integrity was checked with an Agilent Bioanalyzer 2100 (Agilent Technologies). Then, approximately 2.5 μ g of total RNA was used for library preparation with a TruSeq RNA Sample Prep Kit v2 (Illumina) according to the manufacturer's protocol. The libraries were sequenced with HiSeq2000 (Illumina) in single-read mode, creating reads with a length of 50 bp. Sequencing chemistry v2 (Illumina) was used, and samples were multiplexed in three samples per lane. The sequencing approach resulted in around 30–45 million reads per sample. RNA-seq reads of 50 bp were mapped to the mouse genome (mm9) with TopHat2 (Langmead et al., 2009; Trapnell et al., 2009, 2012). Subsequent differential expression analysis was performed by Cufflinks2 (Trapnell et al., 2010) according their protocol (Trapnell et al., 2012). Fragments per kilobase per million mapped reads was calculated as the expression value for each transcript. Gene ontology and Kyoto encyclopedia of genes and genomes (KEGG) pathway enrichment analysis were performed by dropping the up- and downregulated gene lists into the database for annotation, visualization, and integrated discovery programs (Huang et al., 2009a, 2009b), respectively.

ACCESSION NUMBERS

The NCBI Gene Expression Omnibus accession number for the RNA-seq data reported in this paper is GSE43650.

SUPPLEMENTAL INFORMATION

Supplemental Information contains Supplemental Experimental Procedures, seven figures, and two tables and can be found with this article online at <http://dx.doi.org/10.1016/j.stem.2014.04.001>.

ACKNOWLEDGMENTS

We thank L. Frappart for the advice and the discussion on histological analysis and A. Saidi and P.-O. Frappart for their help in the project. We are grateful to M. Baldauf for his histological assistance and A. Krueger for her technical support. We also thank C. Mueller and M. Rodriguez for their excellent assistance in the maintenance of the animal colonies. We are also grateful to many other members of our laboratory for the helpful discussions. A.T. was supported by a postdoc fellowship of the Leibniz Institute for Age Research (FLI), and Z.-W.Z. was a student of the Graduate School on Ageing (LGSA). P.W. is a recipient of the Student Fellowship from the China Scholarship Council. Z.-Q.W. is supported in part by the Deutschen Forschungsgemeinschaft (DFG).

Received: April 15, 2013

Revised: January 12, 2014

Accepted: March 31, 2014

Published: May 1, 2014

REFERENCES

Alarcón, J.M., Malleret, G., Touzani, K., Vronskaya, S., Ishii, S., Kandel, E.R., and Barco, A. (2004). Chromatin acetylation, memory, and LTP are impaired in CBP[±] mice: a model for the cognitive deficit in Rubinstein-Taybi syndrome and its amelioration. *Neuron* **42**, 947–959.

Arai, Y., Pulvers, J.N., Haffner, C., Schilling, B., Nüsslein, I., Calegari, F., and Huttner, W.B. (2011). Neural stem and progenitor cells shorten S-phase on commitment to neuron production. *Nat Commun* **2**, 154.

Ayoub, A.E., Oh, S., Xie, Y., Leng, J., Cotney, J., Dominguez, M.H., Noonan, J.P., and Rakic, P. (2011). Transcriptional programs in transient embryonic zones of the cerebral cortex defined by high-resolution mRNA sequencing. *Proc. Natl. Acad. Sci. USA* **108**, 14950–14955.

Balasubramanian, V., Boddeke, E., Bakels, R., Küst, B., Kooistra, S., Veneman, A., and Copray, S. (2006). Effects of histone deacetylation inhibition on neuronal differentiation of embryonic mouse neural stem cells. *Neuroscience* **143**, 939–951.

Betz, U.A., Vosschenrich, C.A., Rajewsky, K., and Müller, W. (1996). Bypass of lethality with mosaic mice generated by Cre-loxP-mediated recombination. *Curr. Biol.* **6**, 1307–1316.

Bracken, A.P., Ciro, M., Cocito, A., and Helin, K. (2004). E2F target genes: unraveling the biology. *Trends Biochem. Sci.* **29**, 409–417.

Cooper-Kuhn, C.M., Vroemen, M., Brown, J., Ye, H., Thompson, M.A., Winkler, J., and Kuhn, H.G. (2002). Impaired adult neurogenesis in mice lacking the transcription factor E2F1. *Mol. Cell. Neurosci.* **21**, 312–323.

Dugan, K.A., Wood, M.A., and Cole, M.D. (2002). TIP49, but not TRRAP, modulates c-Myc and E2F1 dependent apoptosis. *Oncogene* **21**, 5835–5843.

Farkas, L.M., and Huttner, W.B. (2008). The cell biology of neural stem and progenitor cells and its significance for their proliferation versus differentiation during mammalian brain development. *Curr. Opin. Cell Biol.* **20**, 707–715.

Fazio, T.G., Huff, J.T., and Panning, B. (2008). An RNAi screen of chromatin proteins identifies Tip60-p400 as a regulator of embryonic stem cell identity. *Cell* **134**, 162–174.

Fietz, S.A., and Huttner, W.B. (2011). Cortical progenitor expansion, self-renewal and neurogenesis—a polarized perspective. *Curr. Opin. Neurobiol.* **21**, 23–35.

Fietz, S.A., Lachmann, R., Brandl, H., Kircher, M., Samusik, N., Schröder, R., Lakshmanaperumal, N., Henry, I., Vogt, J., Riehn, A., et al. (2012). Transcriptomes of germinal zones of human and mouse fetal neocortex suggest a role of extracellular matrix in progenitor self-renewal. *Proc. Natl. Acad. Sci. USA* **109**, 11836–11841.

Frappart, P.O., Tong, W.M., Demuth, I., Radovanovic, I., Herceg, Z., Aguzzi, A., Digweed, M., and Wang, Z.Q. (2005). An essential function for NBS1 in the prevention of ataxia and cerebellar defects. *Nat. Med.* **11**, 538–544.

Frappart, P.O., Lee, Y., Lamont, J., and McKinnon, P.J. (2007). BRCA2 is required for neurogenesis and suppression of medulloblastoma. *EMBO J.* **26**, 2732–2742.

Gal, J.S., Morozov, Y.M., Ayoub, A.E., Chatterjee, M., Rakic, P., and Haydar, T.F. (2006). Molecular and morphological heterogeneity of neural precursors in the mouse neocortical proliferative zones. *J. Neurosci.* **26**, 1045–1056.

Glickstein, S.B., Alexander, S., and Ross, M.E. (2007). Differences in cyclin D2 and D1 protein expression distinguish forebrain progenitor subsets. *Cereb. Cortex* **17**, 632–642.

Glickstein, S.B., Monaghan, J.A., Koeller, H.B., Jones, T.K., and Ross, M.E. (2009). Cyclin D2 is critical for intermediate progenitor cell proliferation in the embryonic cortex. *J. Neurosci.* **29**, 9614–9624.

Götz, M., and Huttner, W.B. (2005). The cell biology of neurogenesis. *Nat. Rev. Mol. Cell Biol.* **6**, 777–788.

Gruber, R., Zhou, Z., Sukchev, M., Joerss, T., Frappart, P.O., and Wang, Z.Q. (2011). MCPH1 regulates the neuroprogenitor division mode by coupling the centrosomal cycle with mitotic entry through the Chk1-Cdc25 pathway. *Nat. Cell Biol.* **13**, 1325–1334.

Han, Y.G., and Alvarez-Buylla, A. (2010). Role of primary cilia in brain development and cancer. *Curr. Opin. Neurobiol.* **20**, 58–67.

Haubensak, W., Attardo, A., Denk, W., and Huttner, W.B. (2004). Neurons arise in the basal neuroepithelium of the early mammalian telencephalon: a major site of neurogenesis. *Proc. Natl. Acad. Sci. USA* **101**, 3196–3201.

Herceg, Z., Hulla, W., Gell, D., Cuenin, C., Leonart, M., Jackson, S., and Wang, Z.Q. (2001). Disruption of Trapp causes early embryonic lethality and defects in cell cycle progression. *Nat. Genet.* **29**, 206–211.

Hirabayashi, Y., and Gotoh, Y. (2010). Epigenetic control of neural precursor cell fate during development. *Nat. Rev. Neurosci.* **11**, 377–388.

Hsieh, J., Nakashima, K., Kuwabara, T., Mejia, E., and Gage, F.H. (2004). Histone deacetylase inhibition-mediated neuronal differentiation of multipotent adult neural progenitor cells. *Proc. Natl. Acad. Sci. USA* **101**, 16659–16664.

Huang, W., Sherman, B.T., and Lempicki, R.A. (2009a). Bioinformatics enrichment tools: paths toward the comprehensive functional analysis of large gene lists. *Nucleic Acids Res.* **37**, 1–13.

- Huang, W., Sherman, B.T., and Lempicki, R.A. (2009b). Systematic and integrative analysis of large gene lists using DAVID bioinformatics resources. *Nat. Protoc.* 4, 44–57.
- Jawerka, M., Colak, D., Dimou, L., Spiller, C., Lagger, S., Montgomery, R.L., Olson, E.N., Wurst, W., Göttlicher, M., and Götz, M. (2010). The specific role of histone deacetylase 2 in adult neurogenesis. *Neuron Glia Biol.* 6, 93–107.
- Juliandi, B., Abematsu, M., and Nakashima, K. (2010). Chromatin remodeling in neural stem cell differentiation. *Curr. Opin. Neurobiol.* 20, 408–415.
- Juliandi, B., Abematsu, M., Sanosaka, T., Tsujimura, K., Smith, A., and Nakashima, K. (2012). Induction of superficial cortical layer neurons from mouse embryonic stem cells by valproic acid. *Neurosci. Res.* 72, 23–31.
- Kriegstein, A.R., and Götz, M. (2003). Radial glia diversity: a matter of cell fate. *Glia* 43, 37–43.
- Lang, S.E., McMahon, S.B., Cole, M.D., and Hearing, P. (2001). E2F transcriptional activation requires TRRAP and GCN5 cofactors. *J. Biol. Chem.* 276, 32627–32634.
- Lange, C., and Calegari, F. (2010). Cdks and cyclins link G1 length and differentiation of embryonic, neural and hematopoietic stem cells. *Cell Cycle* 9, 1893–1900.
- Lange, C., Huttner, W.B., and Calegari, F. (2009). Cdk4/cyclinD1 overexpression in neural stem cells shortens G1, delays neurogenesis, and promotes the generation and expansion of basal progenitors. *Cell Stem Cell* 5, 320–331.
- Langmead, B., Trapnell, C., Pop, M., and Salzberg, S.L. (2009). Ultrafast and memory-efficient alignment of short DNA sequences to the human genome. *Genome Biol.* 10, R25.
- Lee, K.K., and Workman, J.L. (2007). Histone acetyltransferase complexes: one size doesn't fit all. *Nat. Rev. Mol. Cell Biol.* 8, 284–295.
- Li, H., Cuenin, C., Murr, R., Wang, Z.Q., and Herceg, Z. (2004). HAT cofactor Trrap regulates the mitotic checkpoint by modulation of Mad1 and Mad2 expression. *EMBO J.* 23, 4824–4834.
- Loizou, J.I., Oser, G., Shukla, V., Sawan, C., Murr, R., Wang, Z.Q., Trumpp, A., and Herceg, Z. (2009). Histone acetyltransferase cofactor Trrap is essential for maintaining the hematopoietic stem/progenitor cell pool. *J. Immunol.* 183, 6422–6431.
- Martínez-Cerdeño, V., Lemen, J.M., Chan, V., Wey, A., Lin, W., Dent, S.R., and Knöpfler, P.S. (2012). N-Myc and GCN5 regulate significantly overlapping transcriptional programs in neural stem cells. *PLoS ONE* 7, e39456.
- Maurice, T., Duclot, F., Meunier, J., Naert, G., Givalois, L., Meffre, J., Célérier, A., Jacquet, C., Copois, V., Mecht, N., et al. (2008). Altered memory capacities and response to stress in p300/CBP-associated factor (PCAF) histone acetylase knockout mice. *Neuropsychopharmacology* 33, 1584–1602.
- McMahon, S.B., Van Buskirk, H.A., Dugan, K.A., Copeland, T.D., and Cole, M.D. (1998). The novel ATM-related protein TRRAP is an essential cofactor for the c-Myc and E2F oncoproteins. *Cell* 94, 363–374.
- Molyneaux, B.J., Arlotta, P., Menezes, J.R., and Macklis, J.D. (2007). Neuronal subtype specification in the cerebral cortex. *Nat. Rev. Neurosci.* 8, 427–437.
- Montgomery, R.L., Hsieh, J., Barbosa, A.C., Richardson, J.A., and Olson, E.N. (2009). Histone deacetylases 1 and 2 control the progression of neural precursors to neurons during brain development. *Proc. Natl. Acad. Sci. USA* 106, 7876–7881.
- Murr, R., Vaissière, T., Sawan, C., Shukla, V., and Herceg, Z. (2007). Orchestration of chromatin-based processes: mind the TRRAP. *Oncogene* 26, 5358–5372.
- Noctor, S.C., Martínez-Cerdeño, V., and Kriegstein, A.R. (2008). Distinct behaviors of neural stem and progenitor cells underlie cortical neurogenesis. *J. Comp. Neurol.* 508, 28–44.
- Nowakowski, R.S., Lewin, S.B., and Miller, M.W. (1989). Bromodeoxyuridine immunohistochemical determination of the lengths of the cell cycle and the DNA-synthetic phase for an anatomically defined population. *J. Neurocytol.* 18, 311–318.
- Pacey, L.K.K., Stead, S., Gleave, J.A., Tomczyk, K., and Doering, L.C. (2006). Neural stem cell culture: neurosphere generation, microscopical analysis and cryopreservation. *Protocol Exchange*. <http://dx.doi.org/10.1038/nprot.2006.215>.
- Pilaz, L.J., Patti, D., Marcy, G., Ollier, E., Pfister, S., Douglas, R.J., Betizeau, M., Gautier, E., Cortay, V., Doerflinger, N., et al. (2009). Forced G1-phase reduction alters mode of division, neuron number, and laminar phenotype in the cerebral cortex. *Proc. Natl. Acad. Sci. USA* 106, 21924–21929.
- Price, V., Wang, L., and D'Mello, S.R. (2013). Conditional deletion of histone deacetylase-4 in the central nervous system has no major effect on brain architecture or neuronal viability. *J. Neurosci. Res.* 91, 407–415.
- Ravin, R., Hoepfner, D.J., Munno, D.M., Carmel, L., Sullivan, J., Levitt, D.L., Miller, J.L., Athaide, C., Panchision, D.M., and McKay, R.D. (2008). Potency and fate specification in CNS stem cell populations in vitro. *Cell Stem Cell* 3, 670–680.
- Sawan, C., Hernandez-Vargas, H., Murr, R., Lopez, F., Vaissière, T., Ghantous, A.Y., Cuenin, C., Imbert, J., Wang, Z.Q., Ren, B., and Herceg, Z. (2013). Histone acetyltransferase cofactor Trrap maintains self-renewal and restricts differentiation of embryonic stem cells. *Stem Cells* 31, 979–991.
- Shen, Q., Wang, Y., Dimos, J.T., Fasano, C.A., Phoenix, T.N., Lemischka, I.R., Ivanova, N.B., Stifani, S., Morrisey, E.E., and Temple, S. (2006). The timing of cortical neurogenesis is encoded within lineages of individual progenitor cells. *Nat. Neurosci.* 9, 743–751.
- Shull, E.R., Lee, Y., Nakane, H., Stracker, T.H., Zhao, J., Russell, H.R., Petrini, J.H., and McKinnon, P.J. (2009). Differential DNA damage signaling accounts for distinct neural apoptotic responses in ATLD and NBS. *Genes Dev.* 23, 171–180.
- Takahashi, T., Goto, T., Miyama, S., Nowakowski, R.S., and Caviness, V.S., Jr. (1999). Sequence of neuron origin and neocortical laminar fate: relation to cell cycle of origin in the developing murine cerebral wall. *J. Neurosci.* 19, 10357–10371.
- Taubert, S., Gorrini, C., Frank, S.R., Parisi, T., Fuchs, M., Chan, H.M., Livingston, D.M., and Amati, B. (2004). E2F-dependent histone acetylation and recruitment of the Tip60 acetyltransferase complex to chromatin in late G1. *Mol. Cell Biol.* 24, 4546–4556.
- Tiberi, L., Vanderhaeghen, P., and van den Aemeele, J. (2012). Cortical neurogenesis and morphogens: diversity of cues, sources and functions. *Curr. Opin. Cell Biol.* 24, 269–276.
- Trapnell, C., Pachter, L., and Salzberg, S.L. (2009). TopHat: discovering splice junctions with RNA-Seq. *Bioinformatics* 25, 1105–1111.
- Trapnell, C., Williams, B.A., Pertea, G., Mortazavi, A., Kwan, G., van Baren, M.J., Salzberg, S.L., Wold, B.J., and Pachter, L. (2010). Transcript assembly and quantification by RNA-Seq reveals unannotated transcripts and isoform switching during cell differentiation. *Nat. Biotechnol.* 28, 511–515.
- Trapnell, C., Roberts, A., Goff, L., Pertea, G., Kim, D., Kelley, D.R., Pimentel, H., Salzberg, S.L., Rinn, J.L., and Pachter, L. (2012). Differential gene and transcript expression analysis of RNA-seq experiments with TopHat and Cufflinks. *Nat. Protoc.* 7, 562–578.
- Tsai, S.Y., Opavsky, R., Sharma, N., Wu, L., Naidu, S., Nolan, E., Feria-Arias, E., Timmers, C., Opavska, J., de Bruin, A., et al. (2008). Mouse development with a single E2F activator. *Nature* 454, 1137–1141.
- Wang, J., Weaver, I.C., Gauthier-Fisher, A., Wang, H., He, L., Yeomans, J., Wondisford, F., Kaplan, D.R., and Miller, F.D. (2010). CBP histone acetyltransferase activity regulates embryonic neural differentiation in the normal and Rubinstein-Taybi syndrome brain. *Dev. Cell* 18, 114–125.
- Wurdak, H., Zhu, S., Romero, A., Loriger, M., Watson, J., Chiang, C.Y., Zhang, J., Natu, V.S., Lairson, L.L., Walker, J.R., et al. (2010). An RNAi screen identifies TRRAP as a regulator of brain tumor-initiating cell differentiation. *Cell Stem Cell* 6, 37–47.
- Yamauchi, T., Yamauchi, J., Kuwata, T., Tamura, T., Yamashita, T., Bae, N., Westphal, H., Ozato, K., and Nakatani, Y. (2000). Distinct but overlapping roles of histone acetylase PCAF and of the closely related PCAF-B/GCN5 in mouse embryogenesis. *Proc. Natl. Acad. Sci. USA* 97, 11303–11306.
- Zhang, Y., Wang, J., Chen, G., Fan, D., and Deng, M. (2011). Inhibition of Sirt1 promotes neural progenitors toward motoneuron differentiation from human embryonic stem cells. *Biochem. Biophys. Res. Commun.* 404, 610–614.
- Zhou, Z., Bruhn, C., and Wang, Z.Q. (2012). Differential function of NBS1 and ATR in neurogenesis. *DNA Repair (Amst.)* 11, 210–221.

Cell Stem Cell, Volume 15

Supplemental Information

**Trrap-Dependent Histone Acetylation
Specifically Regulates Cell Cycle Gene Transcription
to Control Neural Progenitor Fate Decisions**

Alicia Tapias, Zhong-Wei Zhou, Yue Shi, Zechen Chong, Pei Wang, Marco Groth,
Matthias Platzer, Wieland Huttner, Zdenko Herceg, Yun-Gui Yang, and Zhao-Qi Wang

Supplementary Experimental Procedures

Antibodies used

For NP immunostaining, mouse anti-Nestin (1:500; Millipore) and rabbit anti- β -tubulin III/Tuj1 (1:500; Sigma-Aldrich) antibodies were used. For brain section immunostaining, the following antibodies were used: rat anti-BrdU (1:100; Abcam), rabbit anti-Pax6 (1:30,000; Covance, Princeton, NJ, USA), rabbit anti-Tbr2/Eomes (1:100; Abcam), rat anti-histone H3 (phospho S28) (1:300; Abcam), rabbit anti-Sox2 (1:1,000; Abcam), rabbit anti-Gcn5 (1:100; Santa Cruz Biotechnology, Inc., Santa Cruz, CA, USA) and rabbit anti-CBP (1:100; Santa Cruz Biotech.). For immunoblot, the following antibodies were used: rabbit anti-Trrap (1:1000; kindly provided by S. Jackson (The Gurdon Institute, University of Cambridge, UK)), rabbit anti-E2F-1 C-20 (1:500; Santa Cruz Biotech.), rabbit anti-E2F3 (1:1000; Santa Cruz Biotech.), mouse monoclonal anti-Mad2 (1:1000; BD Biosciences, Franklin Lakes, NJ, USA), mouse monoclonal anti-Cdc25A F-6 (1:500; Santa Cruz Biotech.), rabbit anti-Cyclin A H-432 (1:500; Santa Cruz Biotech.), rabbit anti-Plk1 (1:1000; Abcam, Cambridge, UK), and mouse anti- β -Actin (1:10000; Sigma-Aldrich). The antibodies used for chromatin immunoprecipitation (ChIP) were the following: mouse IgG (Diagenode), rabbit anti-Histone H3 (Abcam), rabbit anti-Acetyl Histone H3 (Millipore, Billerica, MA, USA), rabbit anti-Acetyl Histone H4 (Millipore), rabbit anti-E2F1 (Santa Cruz Biotech.), rabbit anti-E2F3 (Santa Cruz Biotech.), mouse anti-Tip60 (kindly provided by Bruno Amati, Center for Genomic Science of IIT@SEMM, Istituto Italiano di Tecnologia (IIT), Milan, Italy), rabbit anti-Gcn5 (Santa Cruz Biotech.), rabbit anti-PCAF (Cell Signaling, Danvers, MA, USA), rabbit anti-RNA polymerase II CTD repeat YSPTSPS (phospho S2) (Abcam) and mouse anti-Trrap (kindly provided by L. Tora, Institute of Genetics and Molecular and Cellular Biology (IGBMC), Illkirch, France).

Primers used for ChIP

The primers used for the promoter analysis were: Cdc25A Fwd, 5'-CCCTCTTCCTTTCTCCATCC-3'; Cdc25A Rev, 5'-CTGCCTCTGTCTCTGCCTCT-3'; Cyclin

A Fwd, 5'-GGGCATAGAGACACGCCTTT-3', Cyclin A Rev, 5'-GCAGGAGCGTATGGATCTGA-3'; Mad2 Fwd, 5'-CTTTAACCCGTGGTGCAACT-3'; Mad2 Rev, 5'-CAGGCGTAATGAGCCCTAAG-3'; Top2A Fwd, 5'-TCAACCACTTTGCACTTCCA-3'; Top2A Rev, 5'-CGCCTTTTCGAATAAACCAA-3'.

Analysis of Trrap mRNA levels

RNA was isolated from E14.5 cortices and primary neuroprogenitor cultures using the Lipid Tissue Mini Kit (Qiagen, Venlo, Netherlands) and following the manufacturer's instructions. cDNA was synthesized using an Affinity Script Multiple Temperature cDNA Synthesis Kit (Agilent Technologies, Santa Clara, CA, USA). qPCRs were performed using Platinum SYBR Green qPCR SuperMix-UDG and a LightCycler 480 Real-Time PCR System. The primers used for PCR amplification were previously described (Loizou et al., 2009) and were as follows: Trrap: Fwd, 5'-CGGGATCCATGAAGCTTCAC-3'; Rev, 5'-AACTCTCCAGGGATCTCCAC-3'; Actin: Fwd, 5'-AGAGGGAAATCGTGCGTGAC-3'; Rev, 5'-CAATAGTGATGACCTGGCCGT-3'. Quantification of the qPCR data was performed by the $\Delta\Delta C_p$ method using Actin as an internal control. Gene expression values were expressed relative to the gene expression in heterozygous embryos or isolated neuroprogenitors.

Analysis of division plane orientation

Coronal sections were stained with mouse monoclonal N-cadherin antibody (1:200; Becton Dickinson, Franklin Lakes, NJ, USA) to label the apical plasma membrane and identify the 'cadherin hole'. DAPI staining of chromosomes was used to mark the cleavage planes of apical progenitors in anaphase.

Immunofluorescence staining of sections

The following antibodies were used: rabbit anti-Tbr2 (1:100; Abcam), rabbit anti-Sox2 (1:1,000; Abcam), rabbit anti-Cyclin D1 (1:100; Thermo) and rabbit anti-Cyclin D2 (1:50;

Santa Cruz). Briefly, for cyclin D immunostaining, following antigen retrieval using a decloaking chamber and 0.01 M Na citrate, pH 6, for 30 minutes at 120°C and blocking for 30 minutes at room temperature with blocking solution (0.1% BSA, 5% goat serum, 0.4% triton in PBS), cryosections were incubated with the primary antibody diluted in blocking solution overnight at 4°C. Secondary antibodies were also diluted in blocking solution. Sections were counterstained and mounted with Prolong Gold anti-fade reagent.

NP transfection and qRT-PCR analysis

NPs were plated in 24-well plates in adherent conditions and overexpression of E2F1 was achieved by transfection using Lipofectamine 2000 (Invitrogen). The vector pCMVHA-E2F1 used to overexpress E2F1 was a gift from Kristian Helin (Biotech Research and Innovation Centre and Centre for Epigenetics, University of Copenhagen, Denmark). Addgene plasmid #24225). Invitrogen's pcDNA3 empty vector was used as a control. Forty-eight hours after transfection, RNA was isolated from NPs using Tri reagent (Life Technologies). cDNA was synthesized using an Affinity Script Multiple Temperature cDNA Synthesis Kit (Agilent Technologies, Santa Clara, CA, USA). qPCRs were performed using Platinum SYBR Green qPCR SuperMix-UDG and a LightCycler 480 Real-Time PCR System. The primers used for PCR amplification were as follows: E2F1 (Fang et al., 2010): Fwd, 5'-TAGCCCTGGGAAGACCTCAT-3'; Rev, 5'-CCCCAAAGTCACAGTCAAAGAG-3'; Top2A: Fwd, 5'-CACCGCTGCAGCCTGTAAATGA-3'; Rev, 5'-CACATTTGCTGGGTCCTAACTCCAC-3'; Actin: Fwd, 5'-AGAGGGAAATCGTGCGTGAC-3'; Rev, 5'-CAATAGTGATGACCTGGCCGT-3'. Quantification of the qPCR data was performed by the $\Delta\Delta C_p$ method using β -Actin as an internal control. Gene expression values were expressed relative to the gene expression in control cells transfected with empty vector pcDNA3.

Reference:

- Bracken, A. P., Ciro, M., Cocito, A., and Helin, K. (2004). E2F target genes: unraveling the biology. *Trends Biochem Sci* 29, 409-417.
- Loizou, J. I., Oser, G., Shukla, V., Sawan, C., Murr, R., Wang, Z. Q., Trumpp, A., and Herceg, Z. (2009). Histone acetyltransferase cofactor Trrap is essential for maintaining the hematopoietic stem/progenitor cell pool. *J Immunol* 183, 6422-6431.
- Ren, B., Cam, H., Takahashi, Y., Volkert, T., Terragni, J., Young, R. A., and Dynlacht, B. D. (2002). E2F integrates cell cycle progression with DNA repair, replication, and G(2)/M checkpoints. *Genes Dev* 16, 245-256.

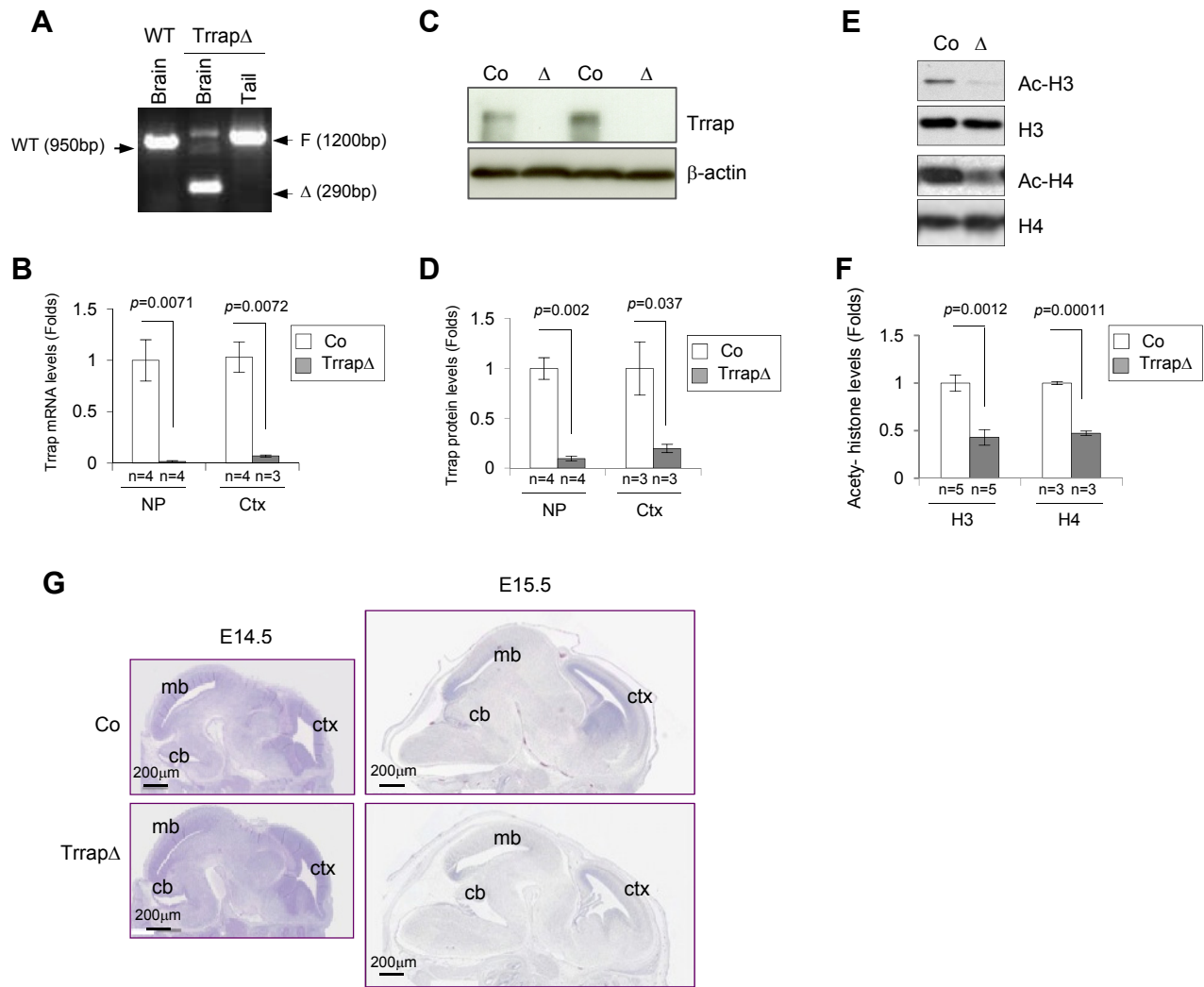


Figure S1 related to Figure 1. Genotyping of Trrap-CNS Δ brains

(A) PCR genotyping of tail and brain tissues of newborn mice. F: floxed, WT: wild type, Δ : deleted.

(B) qPCR analysis of Trrap mRNA levels in control and Trrap-CNS Δ primary cultured NPs and E14.5 cortices using primers directed to the deleted area.

(C) Immunoblot analysis showing efficient deletion of the Trrap protein in brain tissue of Trrap-CNS Δ mice at birth. β -Actin was used as loading control.

(D) Quantification of Trrap protein levels in isolated NPs and E15.5 cortices. β -Actin was used for normalization. Data is expressed as fold change over the protein levels in control samples.

(E) Immunoblot analysis of the acetylation levels of histones H3 and H4.

(F) Quantification of histones H3 and H4 acetylation levels normalized to H3 and H4 levels respectively. Data is expressed as fold change over the acetylation levels in control samples.

(G) H&E staining of sagittal sections from control and Trrap-CNS Δ at the indicated stages.

n = number of embryos analyzed. Mean \pm standard error of mean is shown. Student's *t*-test was performed for statistical analysis. Co: control, Trrap Δ : Trrap-CNS Δ . ctx: cortex, mb: midbrain, cb: cerebellum. NP: primary isolated neuroprogenitors.

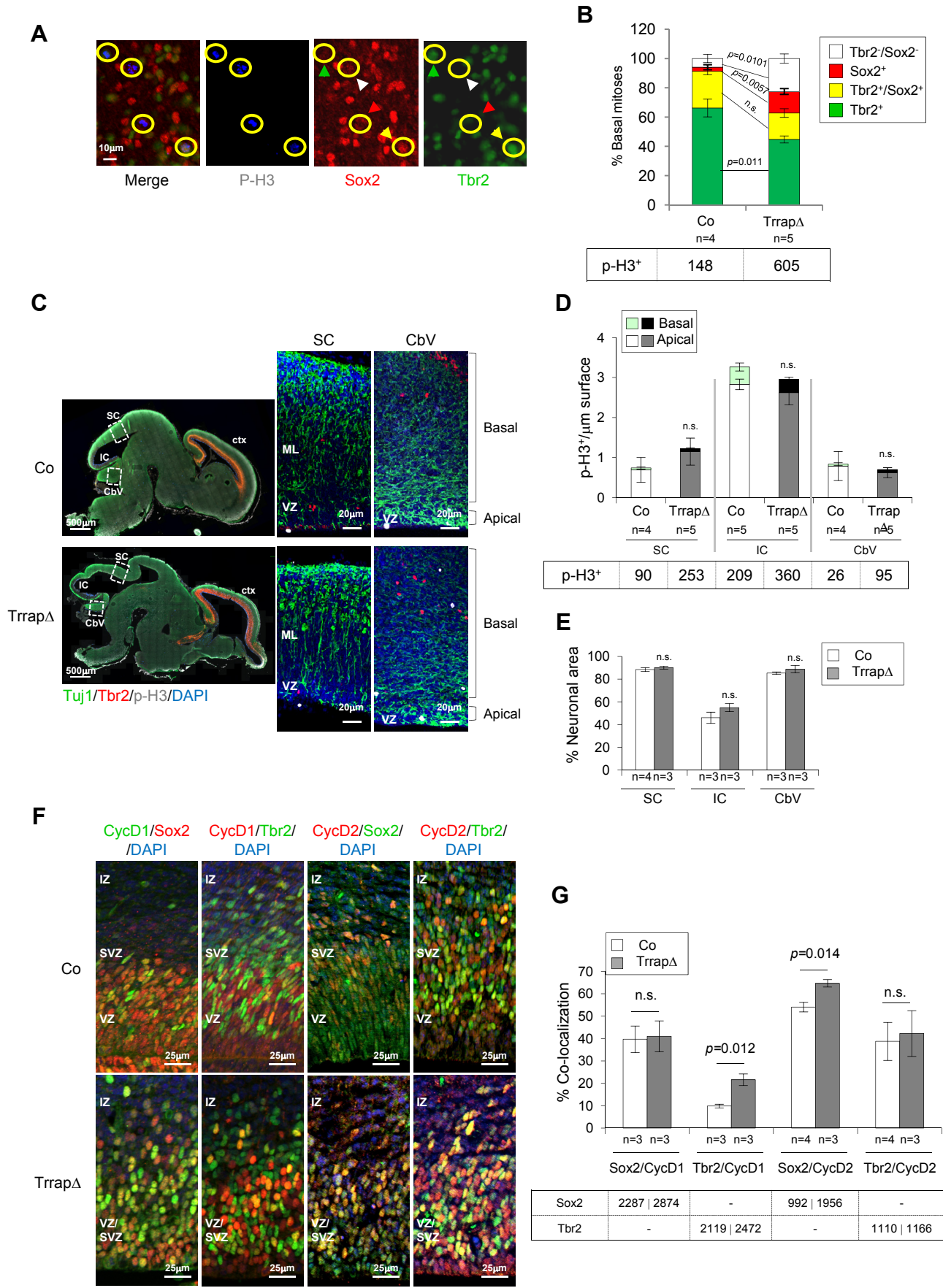


Figure S2

Figure S2 related to Figure 2. Analysis of basal mitoses in Trrap-CNS Δ cortices

(A) Coronal sections of E15.5 embryos were stained against AP marker Sox2 (red), BP marker Tbr2 (green) and mitotic marker p-H3 (blue). Yellow circles indicate basal mitotic cells; red arrow denotes Sox2+Tbr2-mitosis; green arrow indicates Tbr2+ Sox2- mitosis; white arrow denotes Tbr2-Sox2- mitosis; yellow arrow shows double Tbr2+Pax6+ mitosis.

(B) Percentile composition of basal mitotic cells expressing Sox2 and Tbr2 markers, either alone or in combination. Total numbers of p-H3-positive cells from each genotype at E15.5 are listed in the table.

(C) Sagittal sections of E15.5 brains were immunostained with anti-Tbr2 (red), anti-Tuj1 (green) and anti-p-H3 (white) antibodies. Magnification of dashed boxes representing SC and CbV is shown in the right panels.

(D) Quantification of apical and basal mitoses (p-H3+) in the indicated areas is shown. Total numbers of p-H3-positive cells from each genotype are listed in the table.

(E) Quantification of the Tuj1+ area in the indicated brain regions.

(F) Coronal sections of E15.5 embryos were co-stained with antibodies against: Cyclin D1 (green) and Sox2 (red), Cyclin D1 (red) and Tbr2 (green), Cyclin D2 (red) and Sox2 (green) or Cyclin D2 (red) and Tbr2 (green) and counterstained with DAPI (blue).

(G) Quantification of the percentage of co-localization in each staining is shown. Total numbers of scored cells are summarized in the table.

n = number of embryos analyzed. Mean \pm standard error of mean is shown. Student's t-test was performed for statistical analysis. n.s.: not significant. Co: control, Trrap Δ : Trrap-CNS Δ . SC: colliculus superior (midbrain), IC: inferior colliculus (midbrain), CbV: Cerebellar hemisphere (hindbrain), ctx: cortex, VZ: ventricular zone, IZ: intermediate zone, SVZ: subventricular zone, ML: mantle layer.

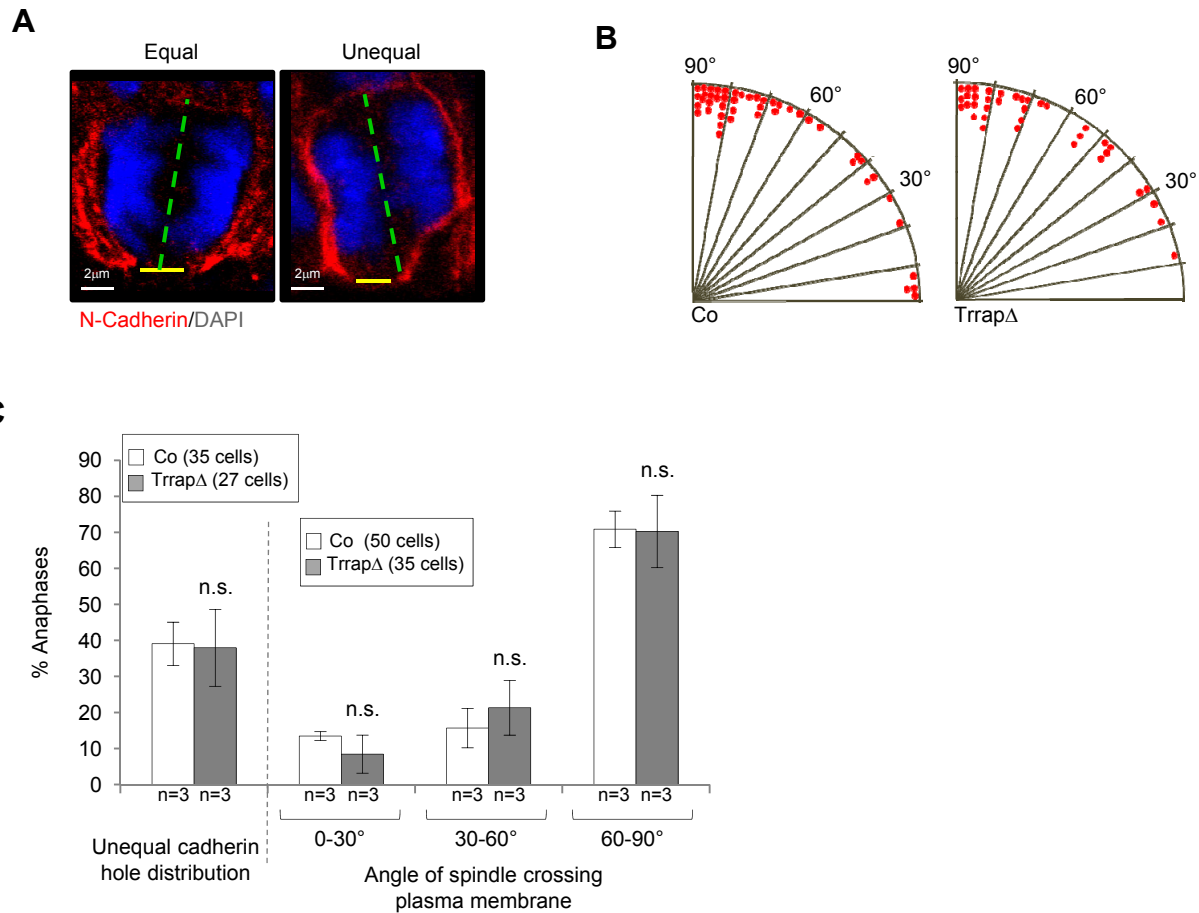


Figure S3 related to Figure 3. In vivo analysis of the cell division mode of neuroprogenitors

(A) Coronal sections were immunostained with anti-N-cadherin (red) to mark the apical plasma membrane and counterstained with DAPI (blue). Examples of E15.5 APs with equal and unequal distribution of the apical plasma membrane in anaphase are shown. Yellow bars represent the ‘cadherin hole’, green dashed lines indicate the cleavage plane of the progenitors in anaphase relative to the ventricular surface according to DAPI staining.

(B) Quantification of cleavage plane orientation of progenitors on the apical surface of the E15.5 cortex. The dots represent each mitotic cell in a given angle range.

(C) The histogram shows the percentage of anaphase progenitors with unequal distribution of the apical plasma membrane (left side) and of anaphase progenitors showing the indicated cleavage plane orientations (right side).

n = number of embryos analyzed. Mean \pm standard error of mean is shown. Student's *t*-test was performed for statistical analysis. *n.s.*: not significant. Co: control, Ttrap Δ : Ttrap-CNS Δ .

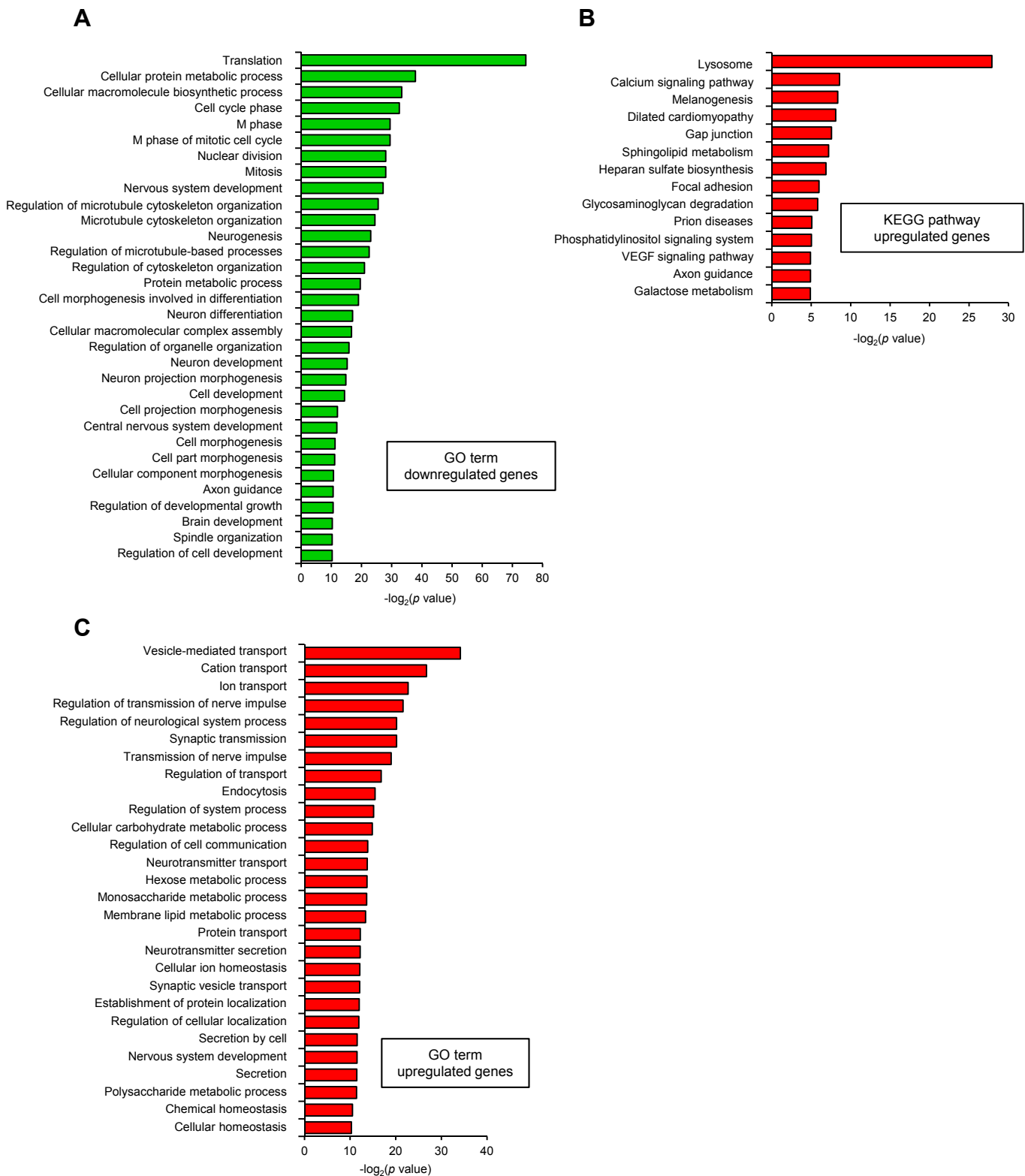


Figure S4 related to Figure 5. Gene Ontology (GO) and KEGG pathway enrichment analysis of the significantly ($q < 0.05$) up- and downregulated genes

(A) Overrepresented GO terms for genes that are downregulated in Ttrap-CNS Δ cortices.

(B) Overrepresented KEGG pathways for genes that are upregulated in Ttrap-CNS Δ cortices.

(C) Overrepresented GO terms for genes that are upregulated in the Ttrap-CNS Δ mouse.

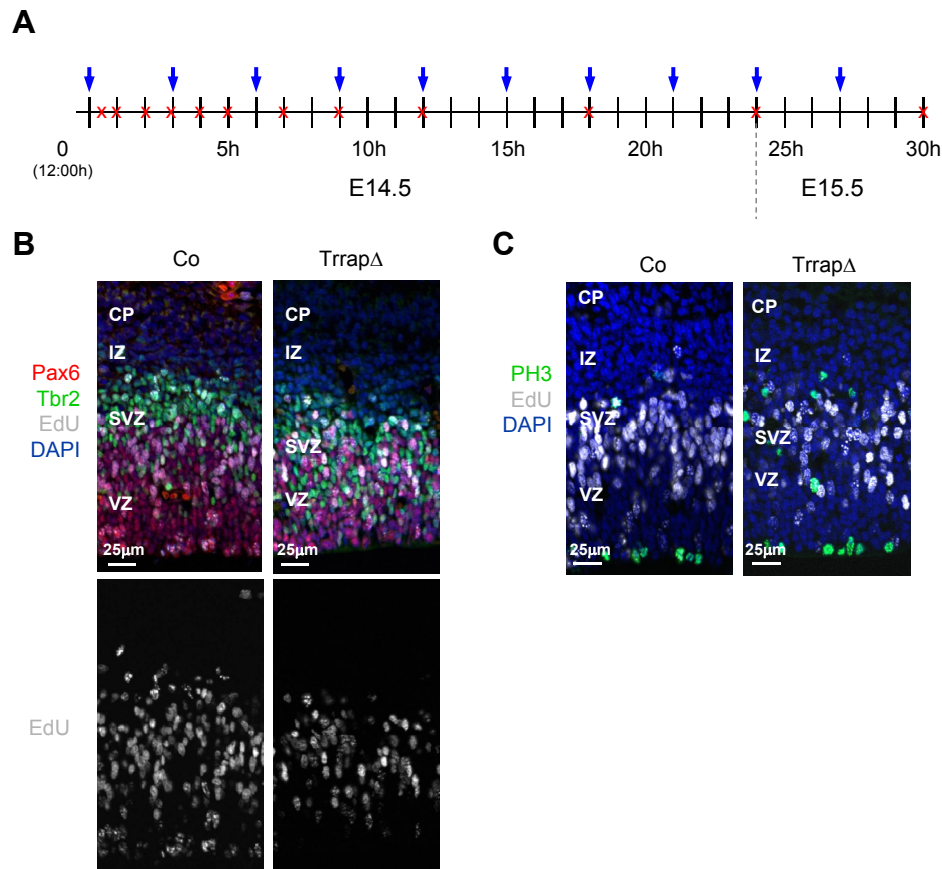


Figure S5 related to Figure 6. Cell cycle analysis of TrrapΔ NPs

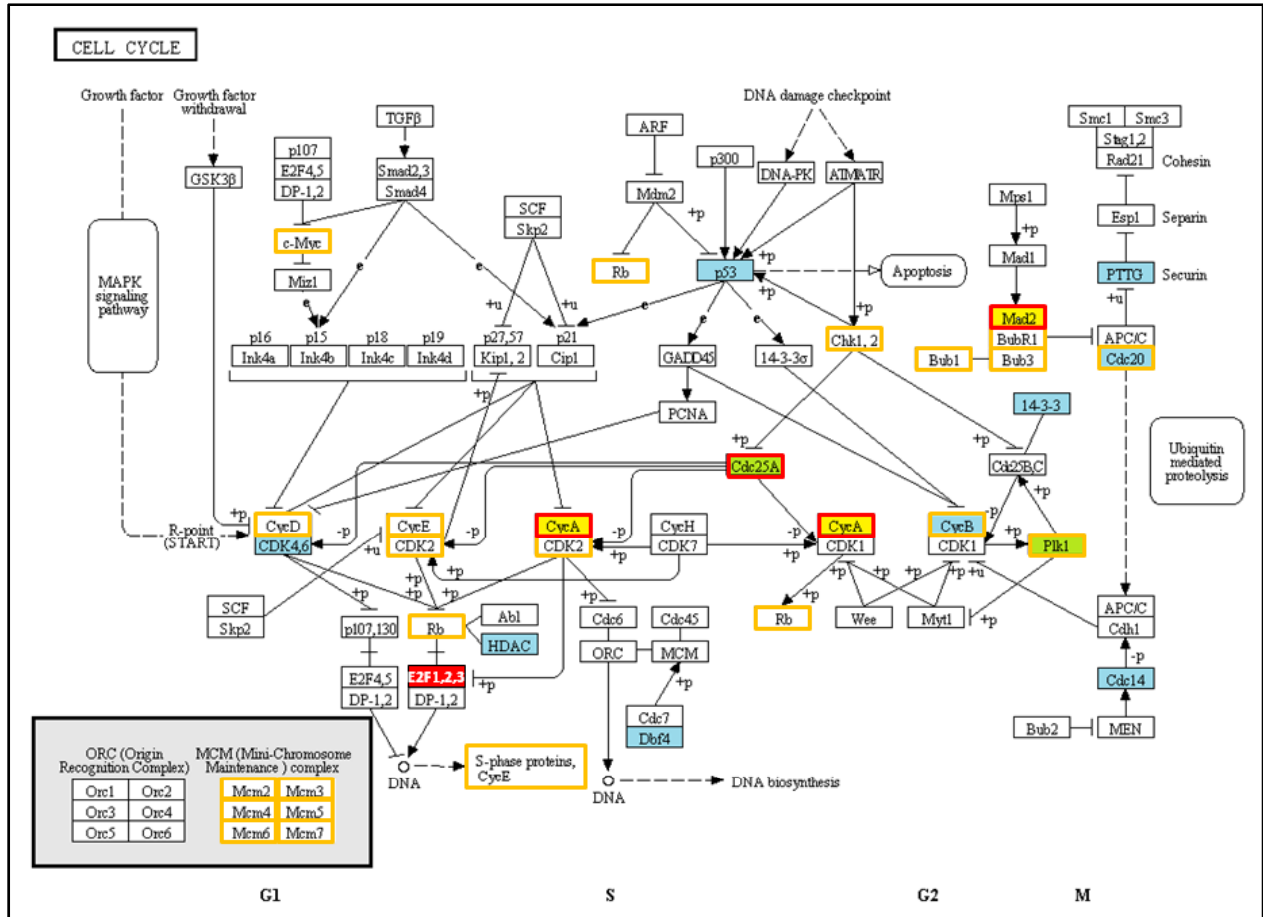
(A) Scheme of the experimental design for cumulative EdU labeling. Blue arrows indicate EdU injections into pregnant mothers every 3 hours. Red crosses denote embryo isolation times between E14.5 and E15.5 stages.

(B) Coronal sections were stained with the AP marker Pax6 (red), the BP marker Tbr2 (green), EdU (gray) and counterstained with DAPI (blue). EdU incorporation after 2 hours is shown as a representative example.

(C) Coronal sections were stained with EdU (gray), the mitotic marker p-H3 (green) and counterstained with DAPI (blue). EdU incorporation after 2 hours is shown as a representative example.

n = number of embryos analyzed. Mean \pm standard error of mean is shown. Student's t -test was performed for statistical analysis. *n.s.*: not significant. Co: control, Trrap Δ : Trrap-CNS Δ . CP: cortical plate, IZ: intermediate zone, SVZ: subventricular zone, VZ: ventricular zone.

A



B

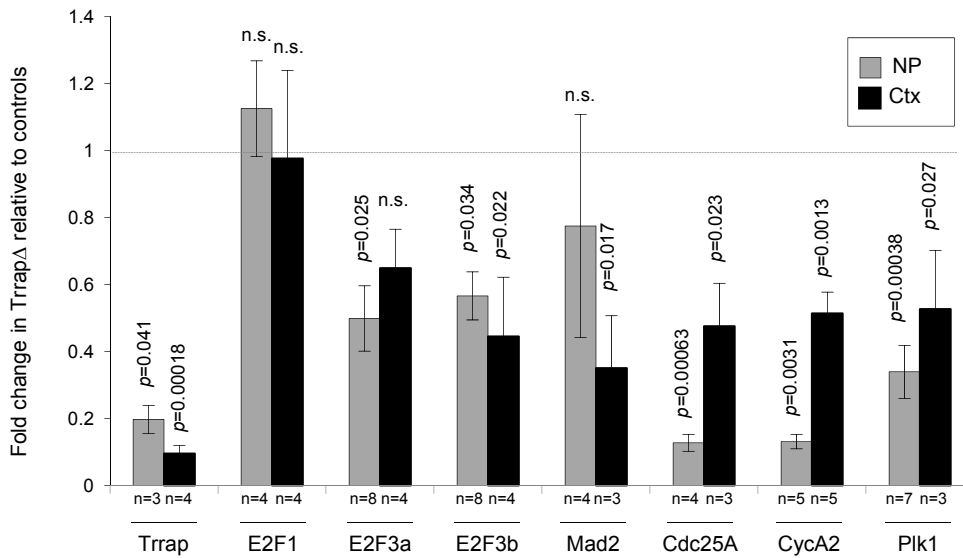


Figure S6

Figure S6 related to Figure 7. Differential expression of E2F targets upon Trrap deletion

(A) Diagram based on the Cell Cycle pathway in the KEGG pathway database. A list of DEGs was imported into Advanced Pathway Painter v2.29 software to generate a cellular pathway map with cell cycle regulators. Yellow and red framed boxes indicate E2F targets. Non-filled boxes indicate non-DEGs. Blue filled boxes represent downregulated genes upon Trrap deletion according to the RNA-seq analysis. Green filled boxes represent genes that were found to be downregulated after Trrap deletion in the RNA-seq analysis, which was confirmed by immunoblotting. Yellow filled boxes denote E2F target genes that despite not being found to be downregulated in the RNA-seq data, their protein levels were determined by immunoblotting to be decreased after Trrap deletion (see Figure 7A). Red framed boxes indicate E2F targets demonstrated by CHIP to exhibit decreased E2F binding after Trrap deletion.

(B) Quantification of protein levels of E2F1 and E2F targets E2F3, Mad2, Cdc25A, Cyclin A, and Plk1 in isolated E14.5 NPs and E15.5 cortices (Ctx) depicted in Figure 7A. β -Actin was used for normalization. Data is expressed as fold change over the protein levels in control samples. n = number of samples analyzed. Mean \pm standard error of mean is shown. Student's t-test was performed for statistical analysis. n.s.: not significant.

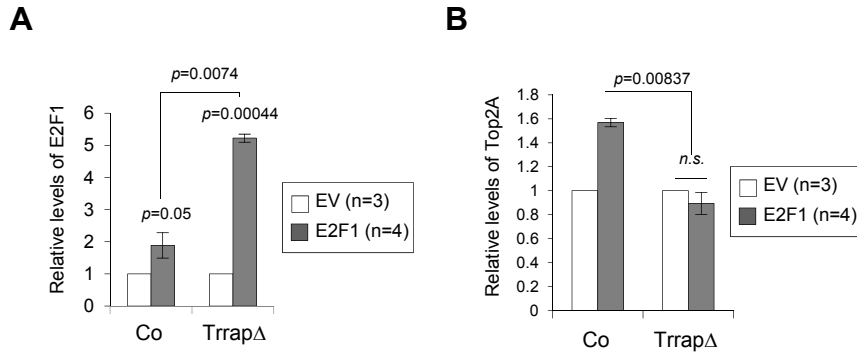


Figure S7 related to Figure 7. Analysis of the E2F and HATs recruitment into E2F-responsive promoters

(A) qPCR analysis of E2F1 mRNA levels after E2F1 overexpression in E14.5 control and TrrapΔ NPs in culture.

(B) Quantification of Top2A mRNA expression by qPCR upon E2F1 overexpression.

n = number of embryos analyzed. Mean ± standard error of mean is shown. Student's *t*-test was performed for statistical analysis. *n.s.*: not significant. EV: empty vector, Co: control, TrrapΔ: Trrap-CNSΔ.

Supplemental Table Legends

Table S1 related to [Figure 5](#). The list of Gene Ontology (GO) and KEGG pathway enrichment analysis of the significantly ($q < 0.05$) up- and downregulated genes

The list includes the GO or KEGG term, statistical information, and the list of genes in each group divided.

Table S2 related to [Figure 7](#). Effects of Trrap deletion on E2F targets

A list of E2F targets classified by function was elaborated using previously published lists (Bracken et al., 2004; Ren et al., 2002). The list of genes was compared to the genes mapped by the RNA-seq analysis and a new list was constructed. The list includes the expression level of the selected genes in control and Trrap-CNS Δ cortices as well as the results of the statistical analysis.